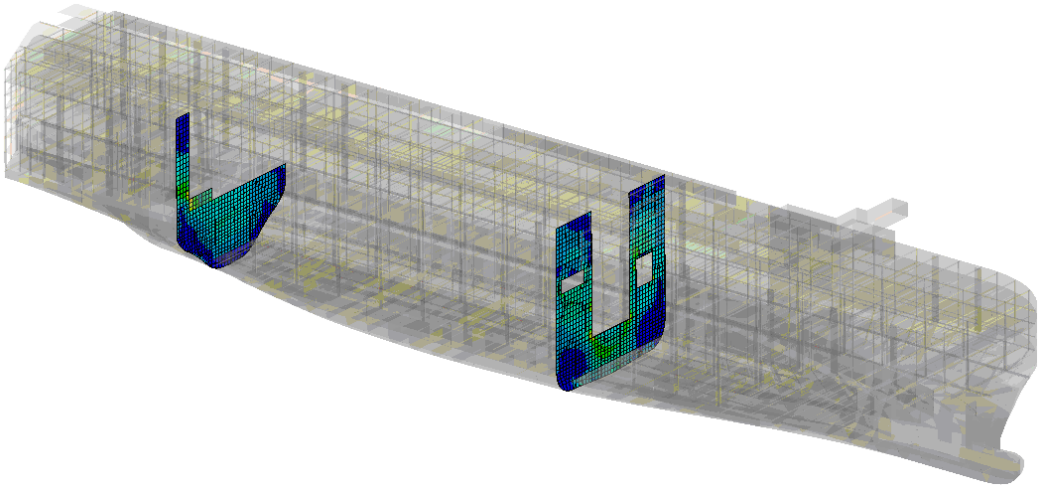

Racking induced stresses in PCTC vessels

M. Sc. Thesis by

CARL-JOHAN SÖDER

March 2008

Centre for Naval Architecture

WALLENIUS OW MARINE

EXECUTIVE SUMMARY

For Pure Car and Truck Carriers (PCTC) the main strength problem is racking. Racking could be described as a global transversal shear force trying to deflect the upper parts of the vessel in athwart direction in relation to the lower hull.

In the first part of this thesis procedures for direct calculations of racking induced stresses have been analyzed. Especially, guidelines regarding racking calculations given by the two classification societies *Lloyd's Register* (LR) and *Det Norske Veritas* (DNV) were evaluated. In order to do so Finite Element (FE) models have been designed and analyzed with properties of typical PCTC vessels. The analysis does include an assessment of strength of the Wallenius Marine vessel PCTC Mignon. Special emphasis has been put on evaluation of the influence from the different boundary conditions that are suggested in the guidelines.

The analysis concluded that stresses in racking constraining structures generally can be assumed to be small when the vessel is upright and that racking induced stresses are mainly caused by transversal motions. The analysis does also conclude that determination of which boundary conditions that are appropriate for a global FE racking analysis do depend of which parts of the vessel that are of interest. For example if the whole vessel is of particular interest a complete global FE model is required. Preferably the racking forces in such analysis should be balanced with a distributed pressure and moment on the submerged hull (DNV-approach). If only the upper parts of the vessel is of interest a limited model (LR approach) extending from the main deck could be a neat and time efficient alternative to a full model. This is due to that these vessels generally are much stiffer in athwart directions below main deck.

In the second part of this thesis a method for monitoring/simulation of racking induced stresses was developed. The method is intended to be used for monitoring of structure as well as for prediction of structures fatigue life. During the analysis the vessel Mignon was used as demonstrator. Mass forces due to motions were applied to a FE model of Mignon. The forces were applied according to the theory of unit loads, coefficients of influence and linear superpositioning.

For time series of motions, hot spot stresses in the racking constraining structure have been simulated for a specific voyage. The simulation was limited to only include inertial and gravitational motions due to roll and sway. The resulting stresses were evaluated against measured stresses obtained from full scale stress measurements onboard the vessel.

Unfortunately the calculated stress levels could not be quantitatively validated against the measured stresses due to a calibration error in the stress measurement system. However, the simulated stresses were shown to be qualitatively consistent with the measured stresses. Hence, the method developed should be appropriate for the simulation of racking induced stresses on PCTC vessels, which for example can be used for monitoring of the fatigue life of structures.

Finally, the stresses in the hot spot locations in the racking frame of Mignon seem to be high. Actually, higher than allowed for classification approval according to the LR strength assessment that was carried out. The simulation of time series does also indicate relatively high stresses even for moderate racking conditions in terms of weather and cargo. Therefore, continuous inspections of these stress locations are recommended.

CONTENTS

INTRODUCTION

BACKGROUND

For Pure Car and Truck Carriers (PCTC) the general strength problem is transverse racking. Racking could be described as a global transversal shear force trying to deflect the upper parts of the vessel in athwart direction in relation to the lower hull.

The ship owner does normally prefer a design with limited transverse bulkheads in the cargo hold in order to provide easy access for the vehicles. With limited transversal bulkhead / web frame structure the transverse deflections of the superstructure relative to lower parts of the hull will increase and so do the stresses.

The general way to analyze racking forces is by FE analysis and various classifications societies and designers uses different analysis approaches. Of special interest in racking analysis is of course the racking constraining structure. This is the structure that is intended to constrain deflections in athwart ship direction. Typical racking constraining structures are transversal bulkheads and engine- and stair casings. Besides these structures the aft part and the fore end of the vessel are important racking constrainers. Racking constraining structures are in many cases unstressed when the ship in upright so the racking induced stresses are mainly due to motions, which implies that fatigue is the general problem.

PURPOSE

One purpose with this work is to compare and evaluate guidelines regarding racking calculations given by the two classification societies *Lloyd's Register* (LR) and *Det Norske Veritas* (DNV). The evaluation is intended to result in suggestions of appropriate calculation models for direct calculations of racking induced stresses.

The aim is also to develop and implement a method for calculation of the local structure responses in the racking constraining structure of PCTC vessels where

- Load cases are formulated based on measured motion responses and are incorporated according to the method of unit loads, coefficients of influence and superpositioning.
- A global FE Model is defined where boundary conditions are determined for a local FE Model where the detailed stress response in the racking constrain structure can be calculated.

The method is intended to be used for monitoring the structure as well as for prediction of structural fatigue life. During the development of the method the Wallenius PCTC Mignon will be used as demonstrator. This is because motion data as well as strain gauge data are available from the vessel. This implies that the structure responses in the calculation model in principle can be checked with reality and consequently will be an important part of the verification of the method.

PCTC MIGNON

The Wallenius Marine PCTC vessel Mignon was built by Daewoo Shipbuilding and Marine Engineering (DSME) in Korea 1999 and elongated with 28,8 meters by Hyundai Vinashin Shipyard in Vietnam 2005. Principal Particulars and General Arrangement are shown in figure 1.

Principal Particulars		
Length overall		227,90 m
Breadth between perpendiculars		219,30 m
Breadth moulded		32,26 m
Depth moulded	(up to freeboard deck)	14,05 m
	(up to upper deck)	33,48 m
Draft moulded	(design)	9,50 m
	(scantling)	11,00 m
Service speed at design draft		20,5 knots

Classification
Lloyd's Register +100A1, Vehicle carrier, movable decks, "Deck no. 4,6 and 8 strengthen for the carriage of Roll on/ Roll off Cargoes"

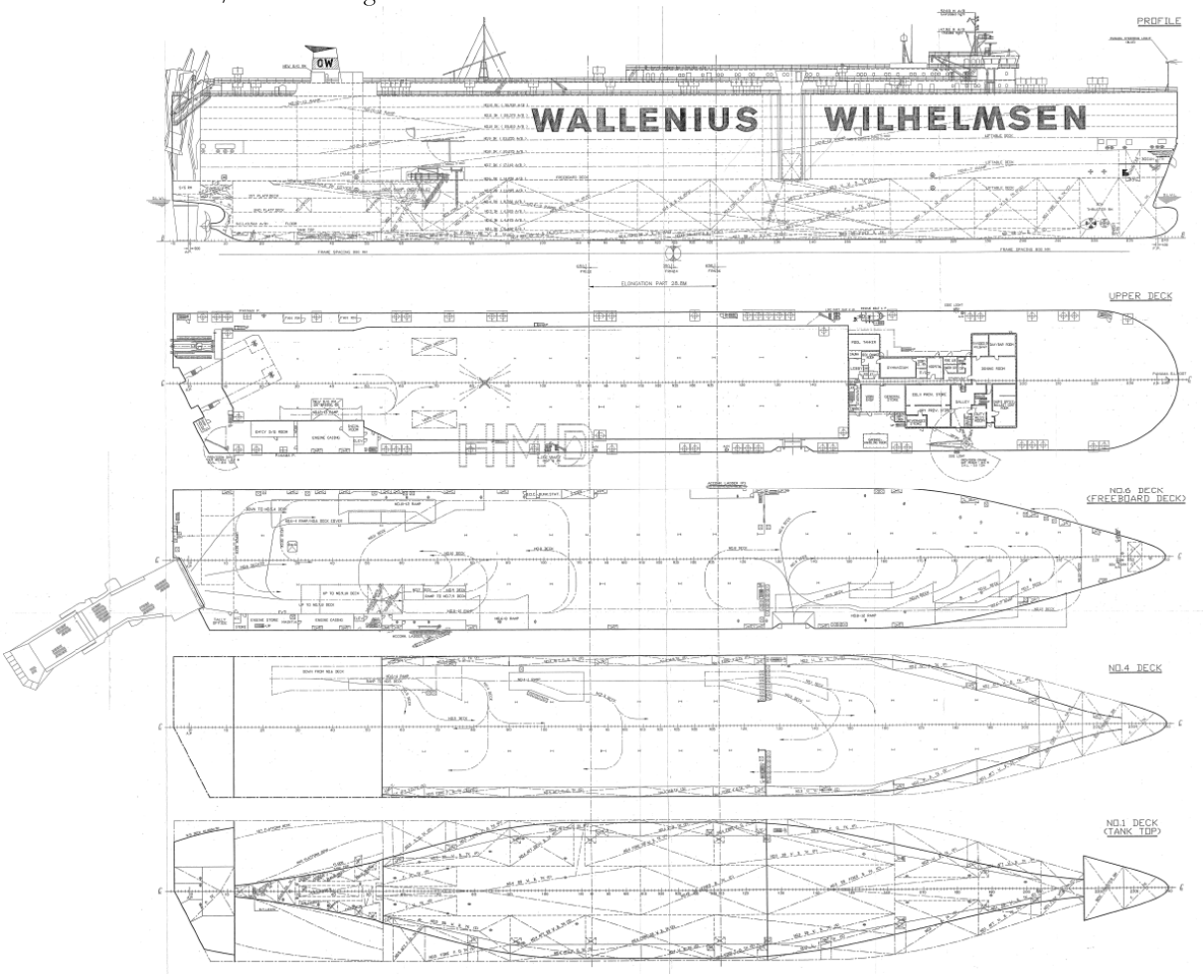

Figure 1, Principal particulars and general arrangement of the PCTC Mignon

Onboard the vessel there are strain gauges installed that measures local stresses in vital positions of the racking constraining structure. There is also a motion recording system installed onboard the vessel. The data recording systems are time synchronized using Global Positioning System (GPS) time. Data from both systems are used during the analysis.

The strain gauges from which data for this analysis will be used are located at the partial bulkhead section (frame no. 126) which is one of the main racking constraining members. In total four gauges are located at the upper corners of the upper openings in the bulkhead. In figure 2 the midship section as well as the partial bulkhead is shown. The gauges (1-4) are mounted in the radiuses and the locations are marked in the figure 2. Further information about the gauges is given in appendix C.

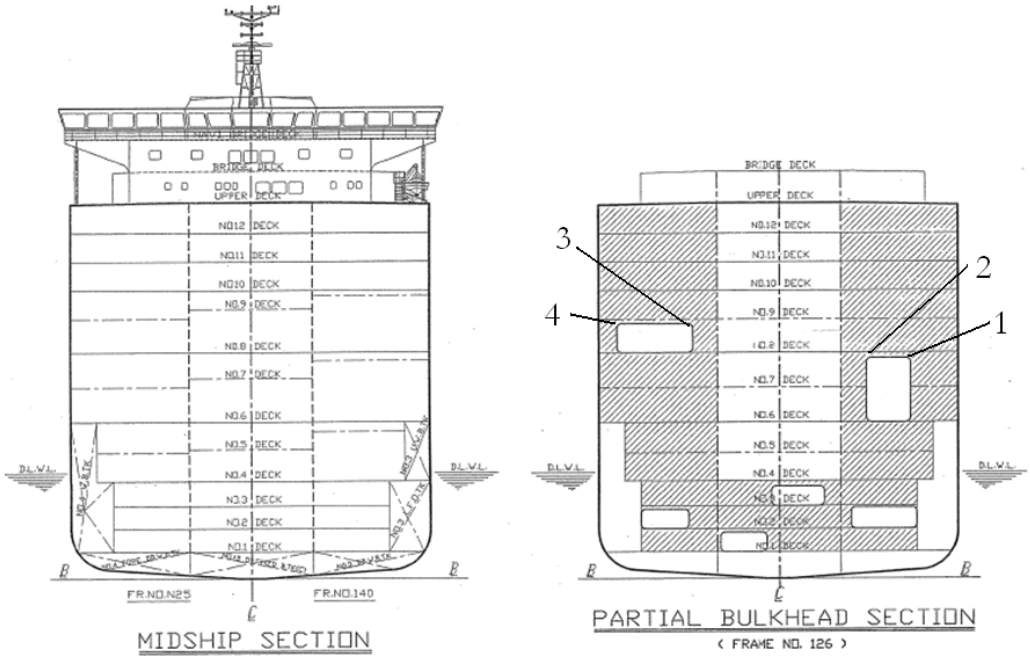

Figure 2, the midship section and partial bulkhead of m/v Mignon seen from fore

Part A: Calculation of Racking Stresses

In this part different procedures for calculation of stresses in racking constraining structures are analysed. In the first section direct calculation guidelines given by two classification societies are studied. Based on this study appropriate calculation models will be suggested and evaluated in the second section. The influences from different loads are also analysed as well as consequences due to simplifications.

Finally a full range calculation model was designed representing Mignon. The model was primarily designed for calculation of deflections and stresses due to racking. In order to compare the different calculation approaches hot spot stresses for the vessel was calculated according to a strength assessment suggested by one of the classification societies.

A.1 CLASS RULES

Various classification societies use different approaches in their guidelines regarding scantling of the racking constraining structure. The common feature is however, to perform a FE analysis mainly based on loads due to rolling. To illustrate the philosophies of the various rules the essence of the classifications notes considering racking given by DNV and LR are described here. In general the rules regarding the structural modelling and meshing are extensive and will be discussed later on in this thesis (Chapter A.3).

A.1.1 DNV CLASSIFICATION NOTES

The classification notes given by DNV [1] require a structure analysis with a global FE model extending over the complete ship. All transverse racking constraining structures should be included in the model. The FE mesh needs to be designed to represent the racking deformation response of the structure. As example of an appropriate global coarse mesh FE model figure 3 is given. Areas of structural significance such as the main racking constraining members may be analysed using a finer mesh model.

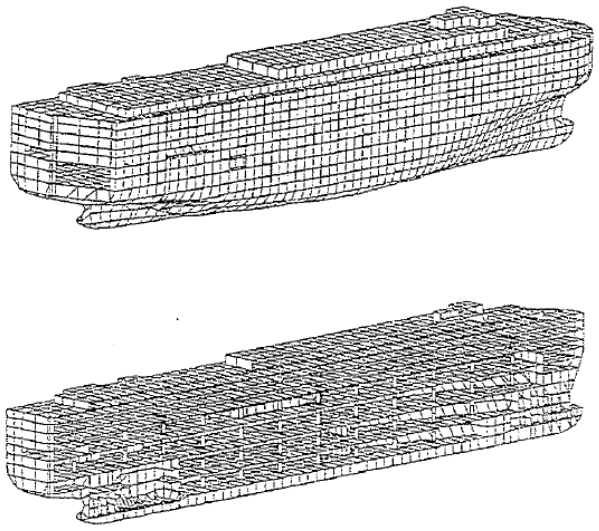

Figure 3, typical appropriate global coarse mesh finite element model of a car carrier according to DNV

The Load cases presented by DNV are rather extensive. The main load case is fatigue governed, therefore all static loads has been disregarded. The main case is a combined load case intended for fatigue assessment for analysis of stresses under combined transverse and vertical loading. Only accelerations and pressure on the submerged hull are applied to the FE model which consists of a fully heavily loaded vessel. The combined load case can be seen in figure 4.

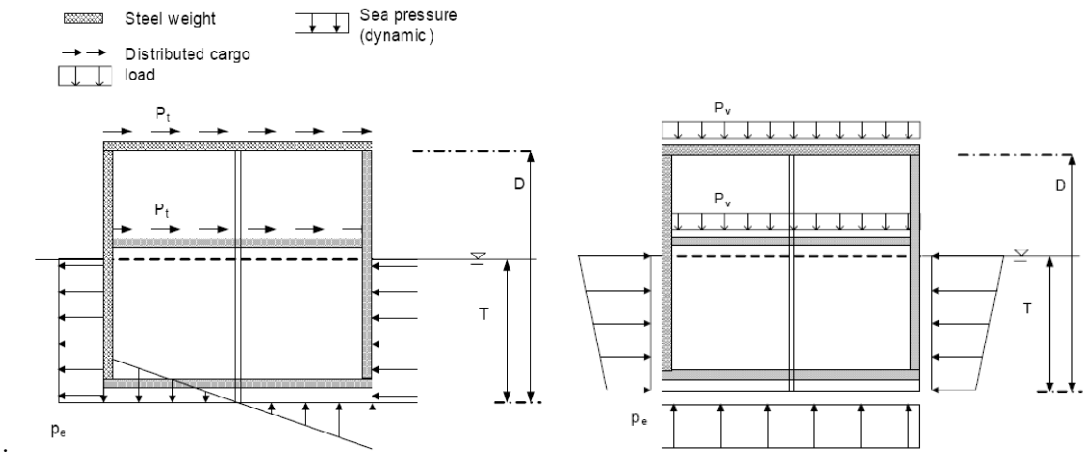

Figure 4, acceleration load case, fatigue governed [1].

The acceleration loads P_t and P_v due to ship motions are determined and applied depending on a large number of characteristic parameters of the vessel like metacentre height, hull dimensions, trade etc. The acceleration applied is typically given as extreme values at a probability level of 10^{-8} and as a reduced value at a probability of 10^{-4}. The forces caused by the transverse acceleration and gravitation are in the model to be balanced with a simplified sea pressure on the submerged hull as can be seen in figure 4.

The outcome from the FE calculation is the structural response at 10^{-8} and 10^{-4} probability levels. The stresses obtained in the first case are to be checked with certain allowable stresses given for extreme cases. The outcome from the second case, stresses at a probability level of 10^{-4}, is used as input to different fatigue assessment procedures.

A.1.2 LR DIRECT CALCULATION PROCEDURE

The procedure given by LR [2] is not as extensive as the DNV procedure, but the analysis still requires a detailed FE model of the vessel. However the model is limited to only extend upwards from the bulkhead deck as shown in figure 5.

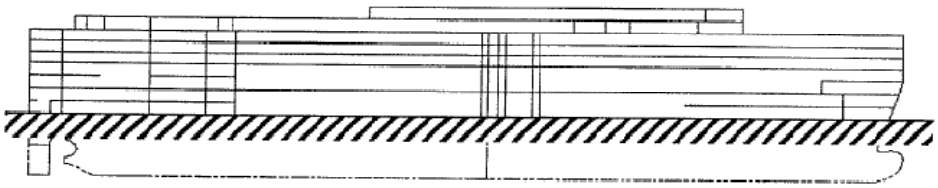

Figure 5, model limitations given by LR extending upwards from the bulkhead deck.

This simplification significantly reduces the work load and is motivated by the fact that these vessels in general are much stiffer below the bulkhead deck. Besides this simplification the structural requirements of the vessel is quite like what is given by DNV, for example all transverse racking constraining structures should be included in the model. The LR procedure does explicitly require the FE procedure to comprise two parts in terms of a global model and local model. The purpose of the local model is to verify the strength of the primary transverse structures using fine mesh models.

The load cases given by LR are quite straight forward and imply a 30 degrees heeled and an upright case. Both load cases should comprise the maximum loading on deck that the ship is designed to carry. Due to the simplification of the model it is to be constrained against both translation and rotation at the level of the bulkhead deck. The structural responses due to these load cases are to be below certain criterion in relation to the yield strength of the material. The LR and DNV procedures will now be compared.

A.2 DUMMY FE MODEL

An accurate way to perform a global FE analysis considering racking is to model the complete vessel, apply inertial and static forces and balance them with hydrostatic pressure on the lower hull. However, such approach is somewhat heavy to manage, i.e. it is time consuming to model the complex structure of the lower body and it is a bit problematic to balance the forces.

An easier approach is to constrain the FE model beneath for example the main deck or the double bottom. Such approach may sound a bit rough but is motivated by the fact that these vessels generally are much stiffer in athwart direction bellow the main deck. Due to this a limited model could be a very neat approach for racking analysis and is as previously seen adapted by LR in their racking analysis guiding lines.

In order to be able to analyze stress deviations due to different boundary conditions and constrains a dummy FE model is constructed in ANSYS [3]. The dummy model is intended to possess the same general properties as the middle part of a typical PCTC vessel. Furthermore, the intention is that different boundary conditions should give similar stress deviations in the dummy model as in a complete FE model. This assumed analogy will be used to analyse which boundary conditions that could be appropriate for a global model in order to reach certain results.

A.2.1 3D MODEL

The dummy model is designed as a 120m constant section as can be seen in figure 6. The model is constructed by assembling 35 identical web frame sections of which every third is a pillar section.
The model does also contain a racking constraining bulkhead frame (racking frame) in the middle, similar to the racking frame in Mignon.

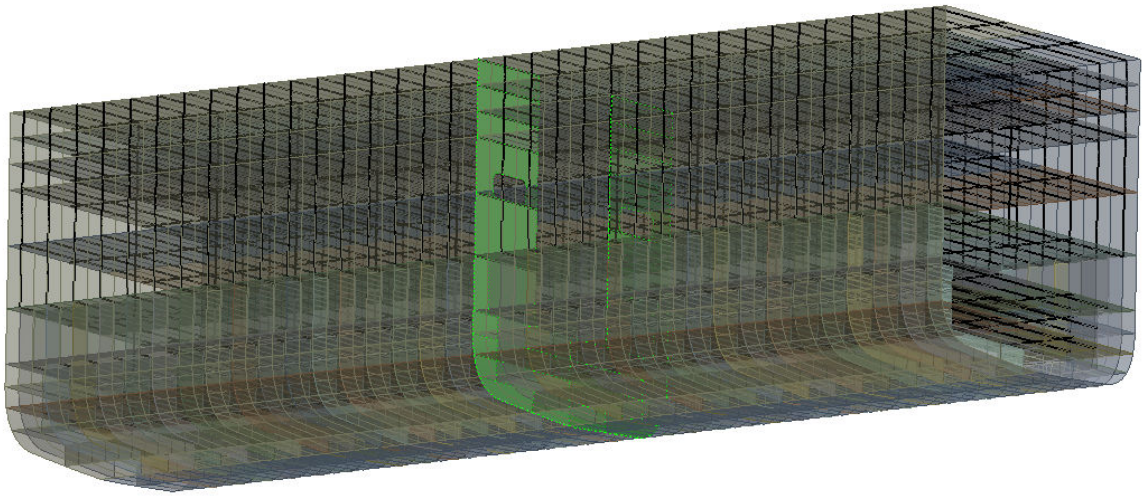

Figure 6, the 3D Finite Element dummy model

Hence, there are three different kinds of transversal sections in the model; the racking frame section, web frame sections and web frame sections with pillars, all can be seen in figure 7.

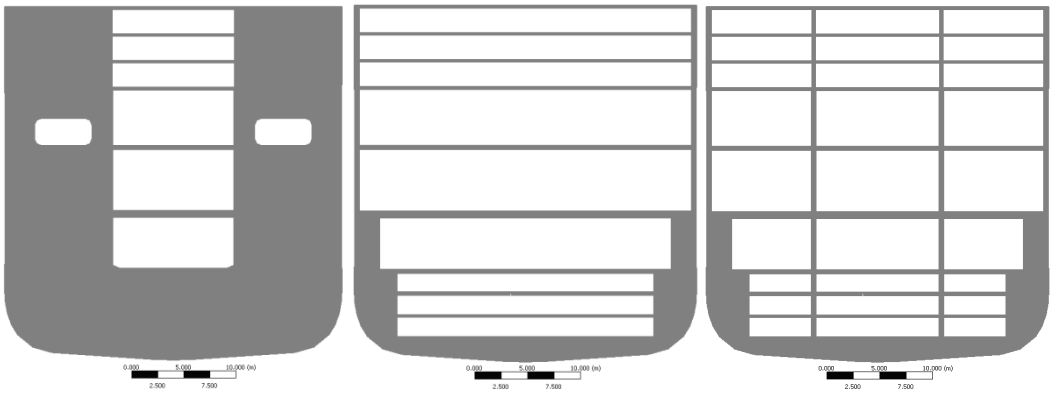

Figure 7, the racking frame section, web frame section and web frame section with pillars.

The deck plates, deck beams, girders and pillars have essentially the same properties as the midship section of Mignon. The web frame spacing is 3,6 meters and the longitudinal pillar spacing is 9,6 meters. The racking frame is similar to the one in Mignon although the plate thickness of the frame is constant (30mm) while it varies from 15 – 40 mm on Mignon. One further simplification is that the shell plates of the vessel have constant thickness (12mm, varies from approximately 10-20 mm on Mignon).

A.2.2 MESH

The mesh in the dummy model is coarse with an average element size of approximately 1 m^2 which can be seen in figure 8. The plating is represented by quadrangular and triangular elements with 4 and 3 nodes respectively. The pillars, girders and deck beams are represented by 2 node beam elements. Worth mentioning is that the same mesh is used for all load cases which is a required condition for an equally premised comparison.

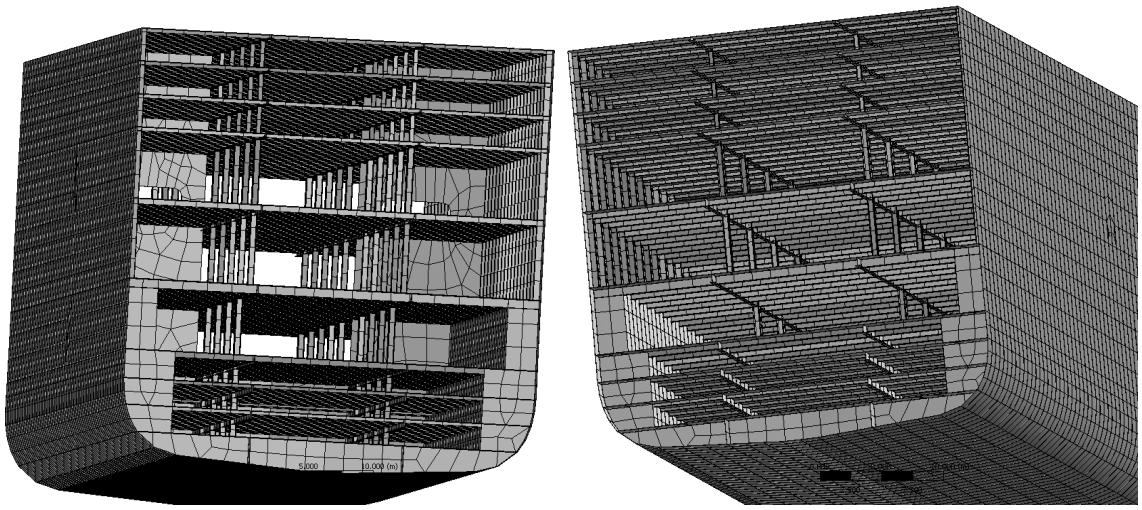

Figure 8, the coarse mesh of the dummy model.

A.2.3 BOUNDARY CONDITION ANALYSIS

Three different boundary conditions have been considered in this analysis. The first case is a balanced case, similar to what is recommended by DNV and the other cases are limited to only extend from the double bottom and deck 6 (LR approach). In each load case a uniform horizontal acceleration of 1 m/s² is affecting the structural weight as seen in figure 9.

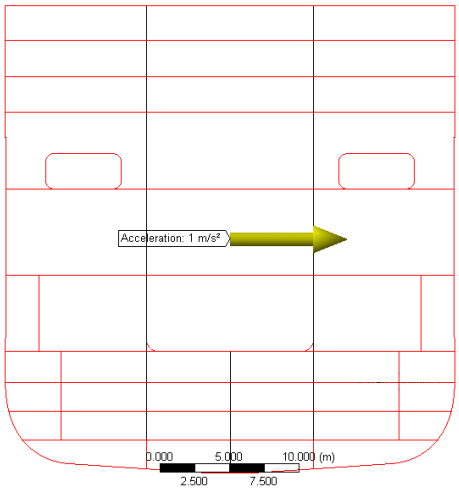

Figure 9, the horizontal acceleration of 1 m/s^2 that is applied in the dummy analysis.

To achieve a balanced model there have to be force as well as moment equilibrium in the FE model. Force equilibrium in athwart direction is obtained by applying a pressure on the lower hull as can be seen in figure 10. The pressure is equally distributed on the projected area normal to the y-direction, below deck 4. Moment equilibrium is obtained by applying a distributed moment on the bottom of the hull as illustrated in figure 10.

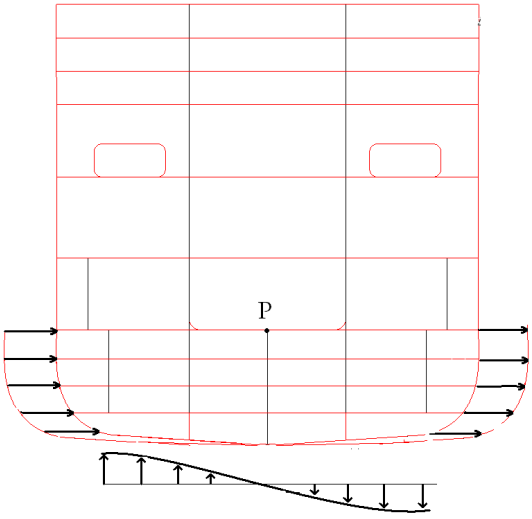

Figure 10, boundary condition 1 where the vessel is balanced.

Perfect balance can not be achieved in the FE simulation so to be able to solve the problem the model is locked at the point P marked in figure 10. But, this point support is not considered to affect the solution since a reaction force of only 30N is obtained in the solution.

The second and third cases which are limited to only extend from the double bottom and deck 6 can be seen in figure 11 and 12 below.

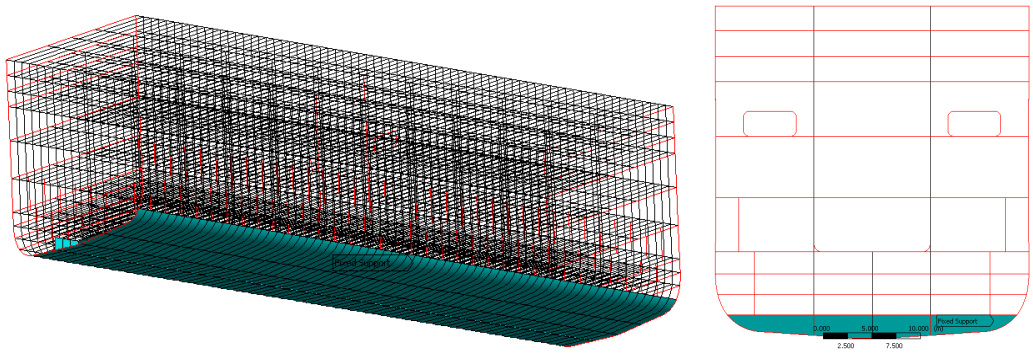

Figure 11, boundary condition 2 where the vessel is clamped below the tank top.

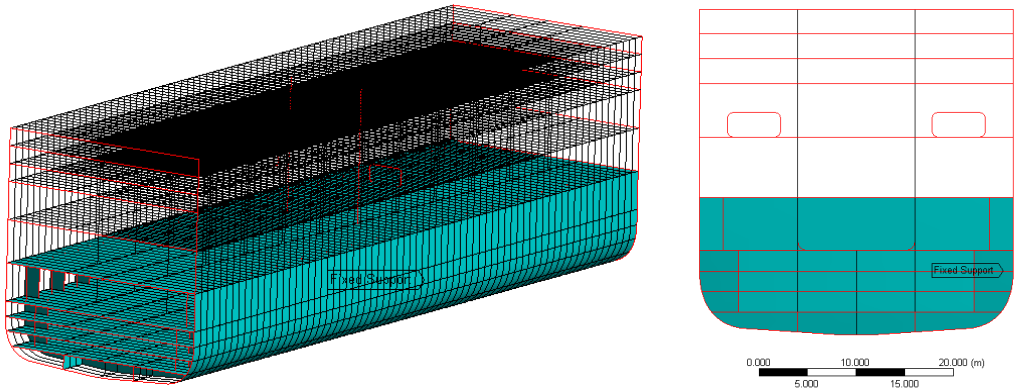

Figure 12, boundary condition 3 where the vessel is clamped below main deck.

To be able to investigate the stress deviations between the different load cases the principal as well as the equivalent stresses (von Mises) were calculated using ANSYS for the different boundary conditions. Of particular interest in this analysis is the racking constraining structure of the model which here is the racking frame. In figure 13, 14 and 15 the principal stresses in the racking frame can be seen illustrated as vectors for all the three cases respectively. The figures show that the stress flow is qualitatively similar in the three different models, when observing the areas around the openings and above. One obvious limitation of the model that is clamped below deck 6 is that every possible critical location is not evaluated

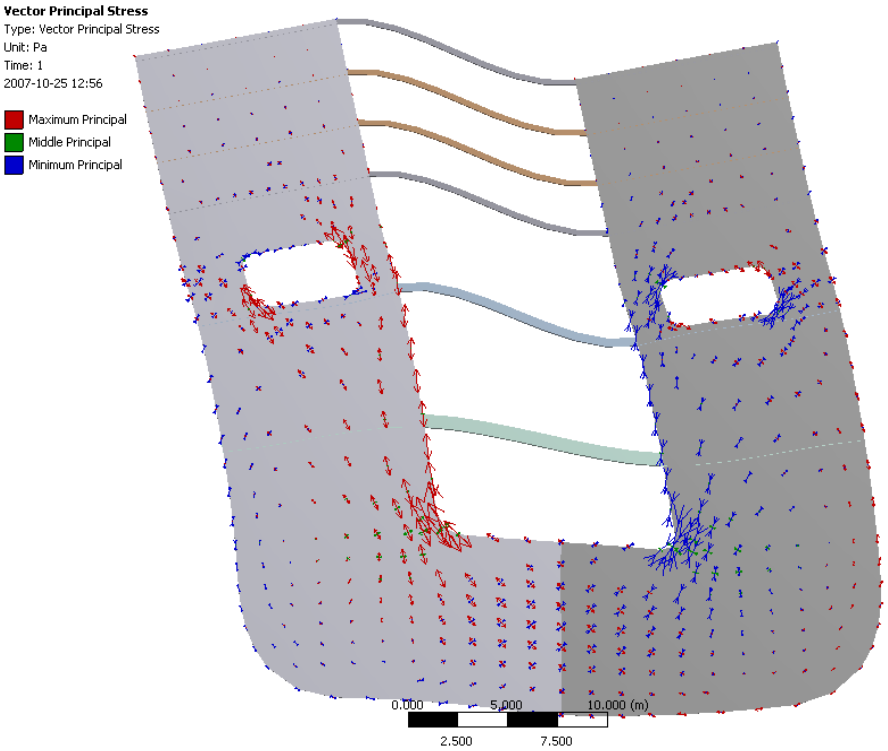

Figure 13, the principal stress vectors in the balanced load case.

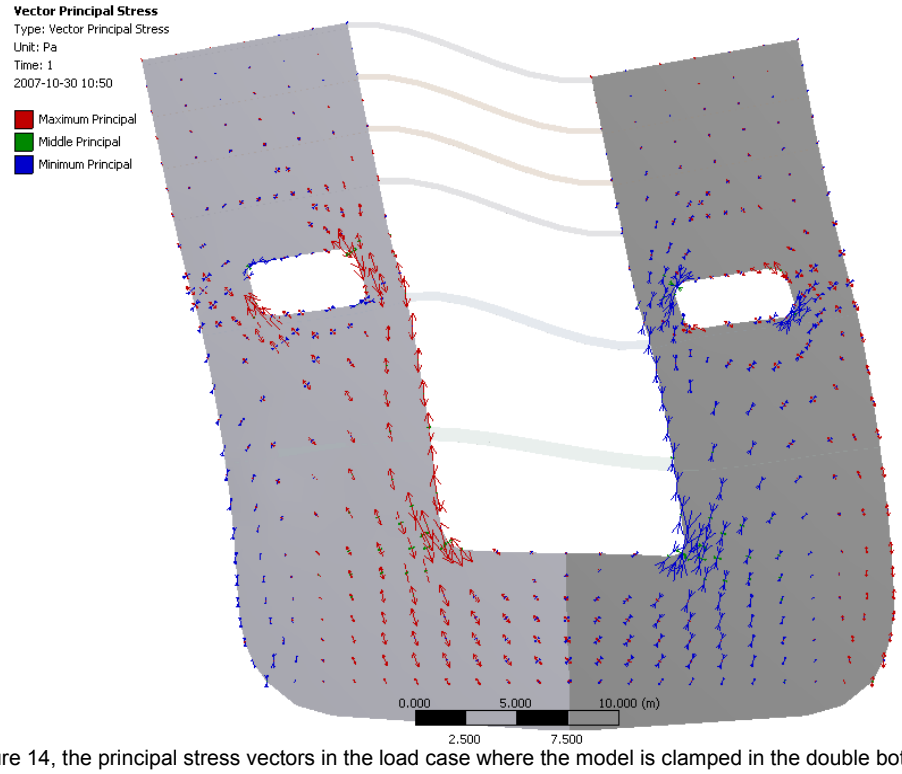

Figure 14, the principal stress vectors in the load case where the model is clamped in the double bottom.

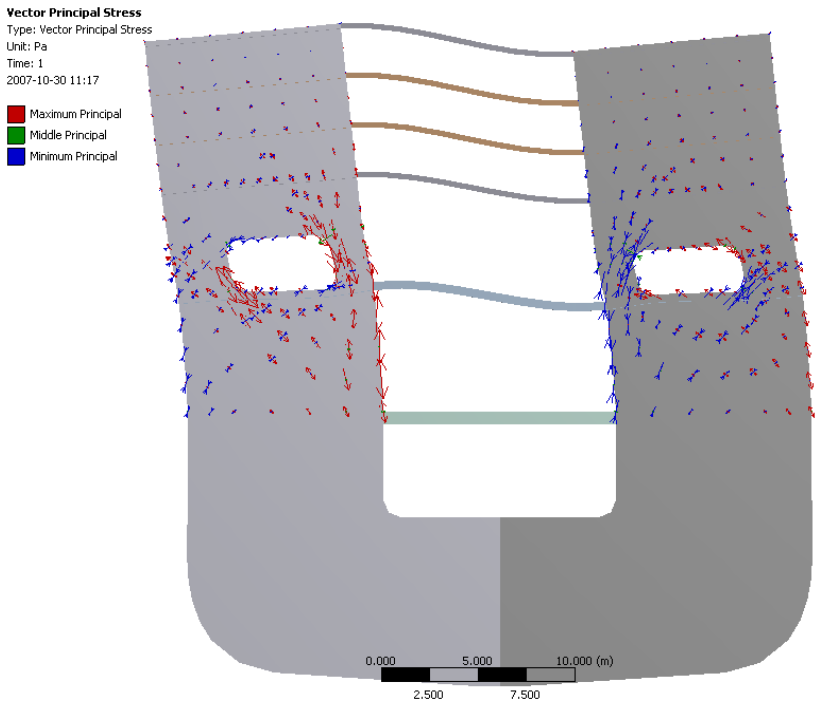

Figure 15, the principal stress vectors in the load case where the model is clamped below deck 6.

To further compare the different load cases the maximum principal stresses above deck 6 are plotted for all three cases in figure 16, 17 and 18. The maximum stress above deck 6 does occur at the same location for all the three different load cases (lower left corner of the left hand opening) which is not all too surprising. However, a bit remarkably is that the result only deviates about 5% between the different cases (25,0MPa, 25,1MPa and 26,0MPa). This indicates that no major stress inaccuracies due to the boundaries are to be expected when analysing these openings if choosing any of these BC.

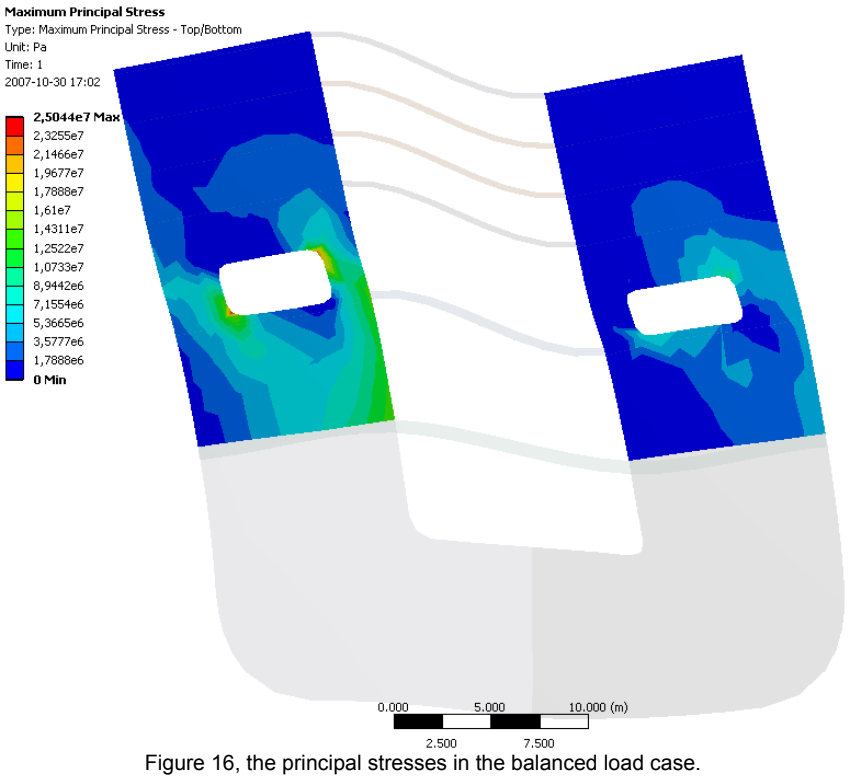

Figure 16, the principal stresses in the balanced load case.

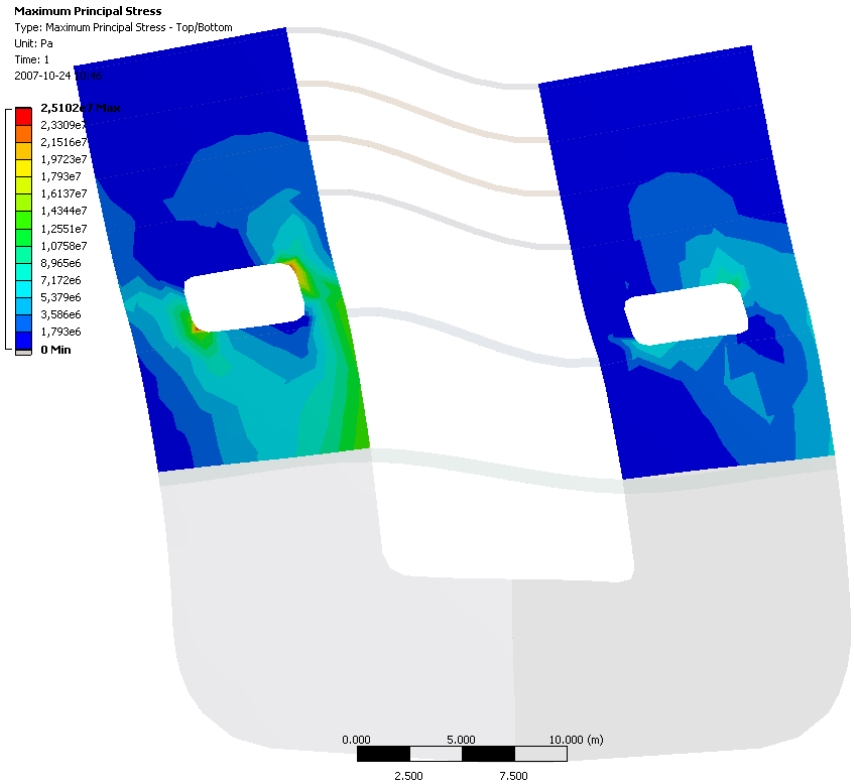

Figure 17, the principal stresses in the load case where the model is clamped below the double bottom.

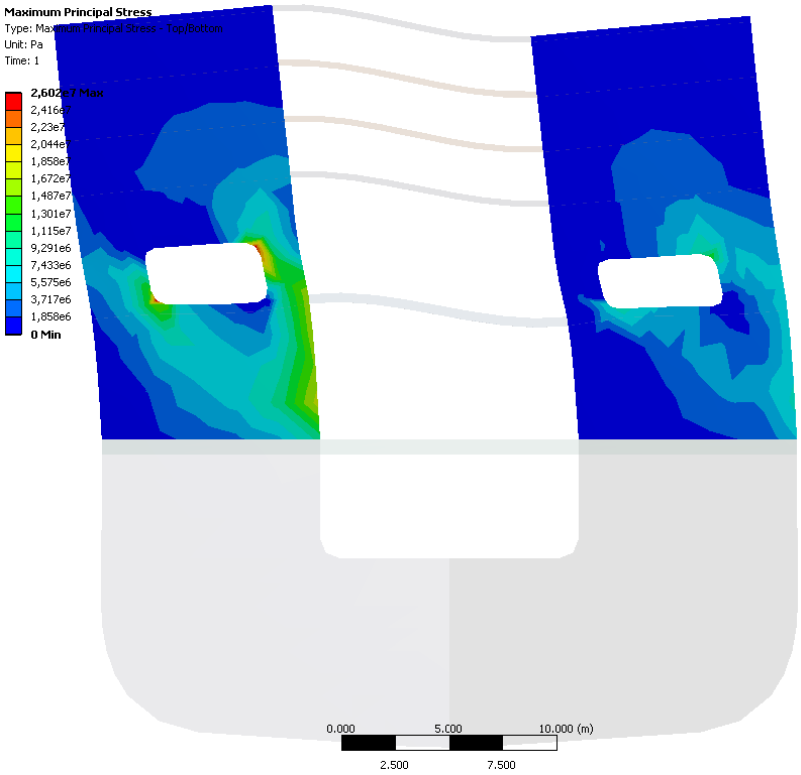

Figure 18, the principal stresses in the load case where the model is clamped below deck 6.

A.2.4 INFLUENCE OF PITCH AND HEAVE ON RACKING CONSTRAINING MEMBERS

Due to the purpose of racking constraining structures stresses should mainly be induced by transversal forces, normally caused by roll and sway motions. This implies that stresses in the racking constraining structure induced by vertical motions of the vessel should be small in comparison to roll and sway induced stresses. To investigate this further the stresses in the racking constraining structure due to vertical acceleration is evaluated using the dummy model. The dummy model is therefore subjected to a vertical acceleration of 1 m/s² (0,1 g) as seen in figure 19. (Please note; the acceleration goes up but the inertial force caused by the acceleration goes down.)

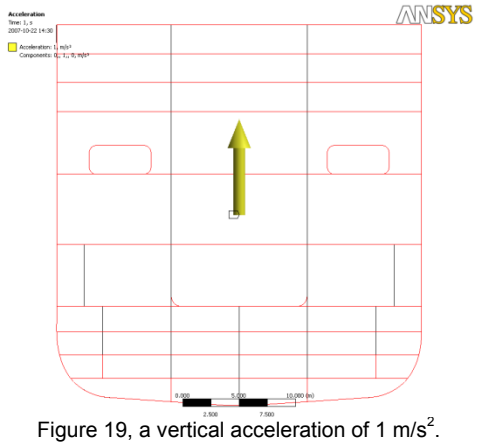

Figure 19, a vertical acceleration of 1 m/s^2.

The stresses in the racking frame are evaluated to compare with the result from the horizontal acceleration cases. The stress distribution in the interesting part of the racking frame can be seen in figure 20. As seen in the figure the highest stress in the racking frame is about 1 MPa.

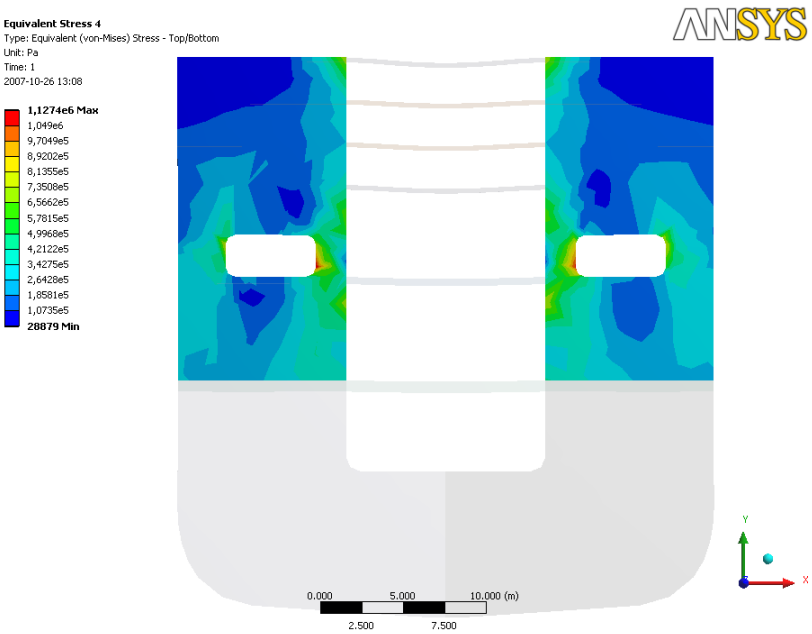

Figure 20, the stresses in the racking frame due to the vertical acceleration of 1 m/s^2 load case.

By judging from these results stresses induced by vertical motions seems to be much smaller than stresses due to roll and sway. Obviously, if the structure was heavily loaded by cargo these stresses would increase but so would also the stresses due to transversal motions do. Also, if multiplying the above stress distribution by a factor 10 the upright stress case is obtained. This shows that stresses in racking constraining structures generally are small when the vessel is in upright position.

A.2.5 CONCLUSIONS

- When performing global racking analysis on PCTC vessels the accurate way to go does unavoidably seem to be to model the complete vessel and to balance the racking forces with some kind of distributed pressure on the lower hull. Such approach is particularly necessary if the whole vessel including the complete hull is of interest. But, if for example the lower hull is of secondary interest a limited model seems to be a neat and time efficient alternative.

- Stresses in racking constraining members due to heave and pitch motion are small compared to roll and sway induced stresses. Motion induced stresses due to heave and pitch will therefore not be considered in the following analysis.

- Stresses in racking constraining structures are generally small when the vessel is upright so stresses in these structures are mainly due to motions, especially transversal motions.

A.3 STRENGTH ASSESSMENT OF PCTC MIGNON

In order to further compare the two classification approaches a full range calculation model is developed using the FE program ANSYS representing the vessel Mignon. The model will in this section be loaded according to the strength assessment given in the LR procedure. The strength assessment load will be applied to a limited "LR boundary" model as well as to a full "DNV boundary" model. In part B the models will also be used for simulation of stresses.

A.3.1 GLOBAL FE MODEL

The global model is intended to represent the overall stiffness and the deflexion pattern for the hull in terms of racking. The modelling is carried out generally following the guidelines given by DNV [1]. This implies that all racking affecting structural members such as external shell, decks, longitudinal and transversal bulkheads, racking constraining girder structures and engine casing are included in the model. An overview of the global model can be seen in figure 21.

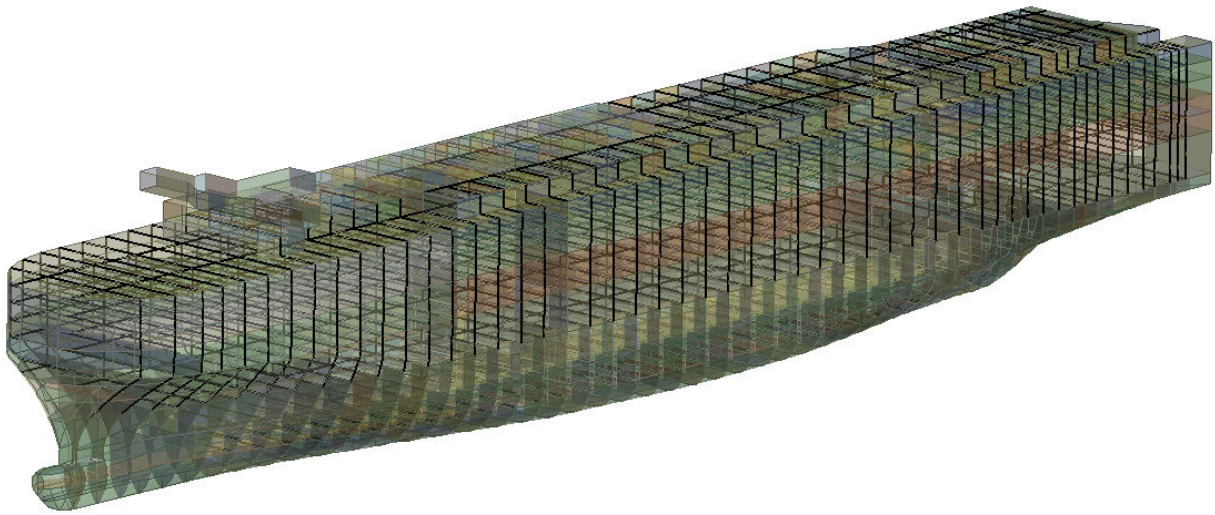

Figure 21, the global FE model of PCTC Mignon

Generally the internal structure has been simplified, especially the lower parts of the fore and aft body. This is due to high complexity of the structure in these parts. The model is however considered to represent the stiffness contribution from these parts in a sufficient way.

Vertical structures represented by shell elements are the shell plating, transom, transverse bulkheads, longitudinal bulkheads, transverse midship "racking" bulkhead and engine casing.

The local stiffeners of the vertical structures (longitudinal and transversal bulkheads and outer shell) are incorporated as added smoothed equivalent area. The estimated equivalent thickness of each vertical structural member is shown in appendix B, table 1.

All transversal structure has been concentrated to the web frame sections (spacing 3200 or 4800mm).
To incorporate that the floor spacing in the double hull generally is half the web spacing the thickness of the floors in the web frames has been doubled. The main transversal and longitudinal bulkheads is shown in figure 22.

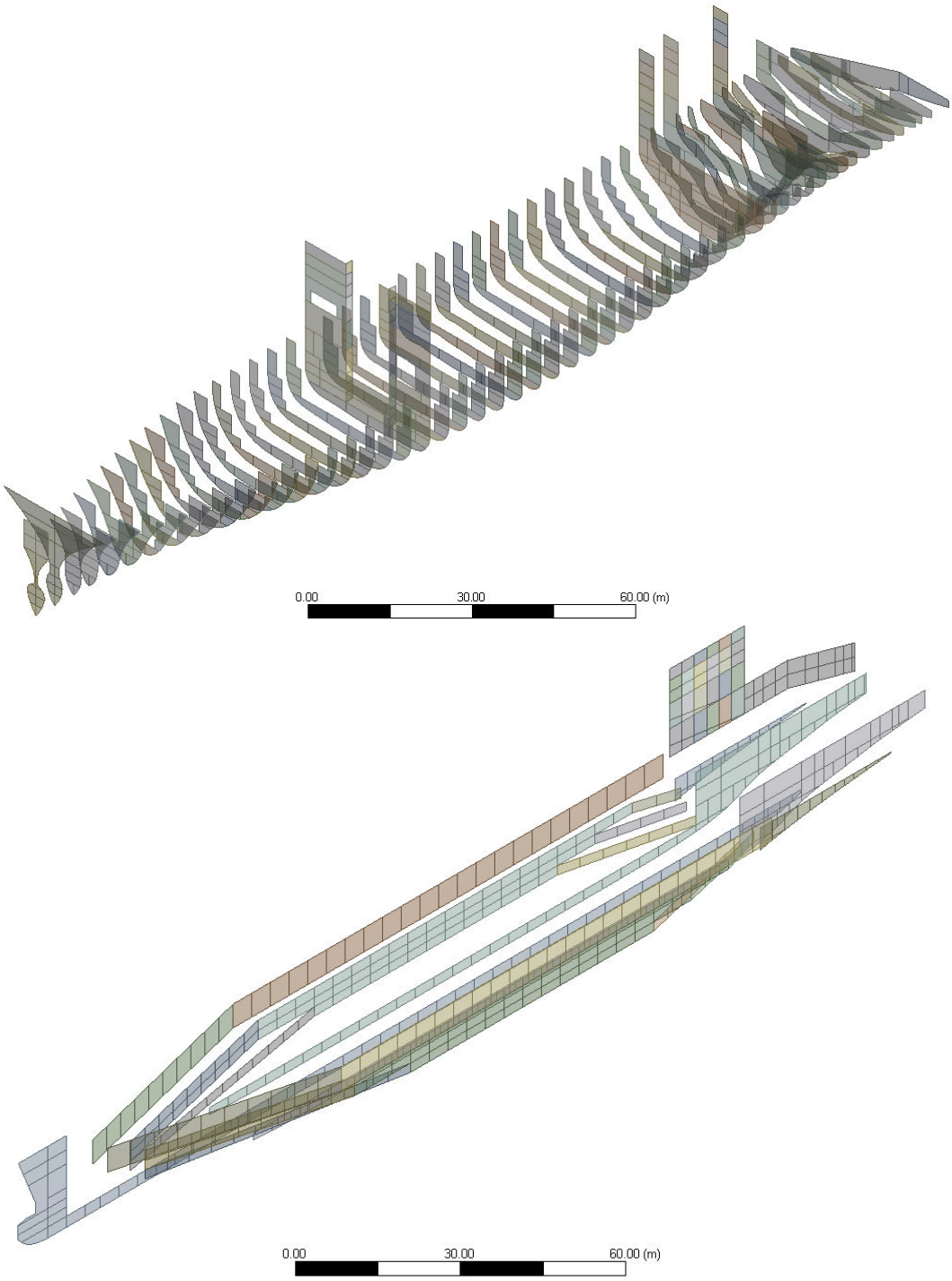

Figure 22, the main transversal as well as the longitudinal bulkheads of the 3D model.

Decks and ramp ways have also been modelled using shell element. The longitudinal stiffeners on the decks are not considered to affect the transversal stiffness of the vessel. But, their contribution to the steel weight of the structure can not be neglected. Therefore the longitudinal stiffeners are incorporated as added density to the decks. The estimated equivalent density of the decks and adjacent ramp ways shown in appendix B, table 2. Weight from movable decks are incorporated as added mass to the nearest fixed deck above.

Only fixed ramp ways between deck 6 and 12 have been modelled. This is due to that the ramp ways below deck 6 are considered to have minor influence on the overall stiffness. Deck and ramp way structure are shown in figure 23.

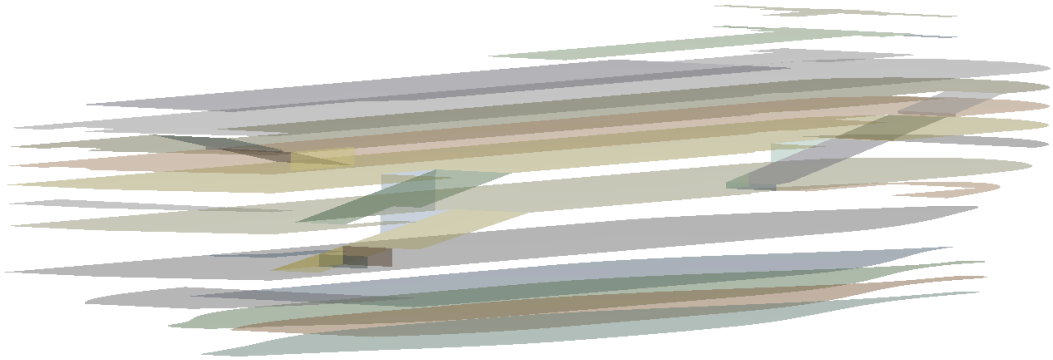

Figure 23, the deck and ramp way structure used in the analysis.

Deck transversals, longitudinal girder, pillars and ventilation ducts have been represented by beam elements in the model. These beams are shown in figure 24.

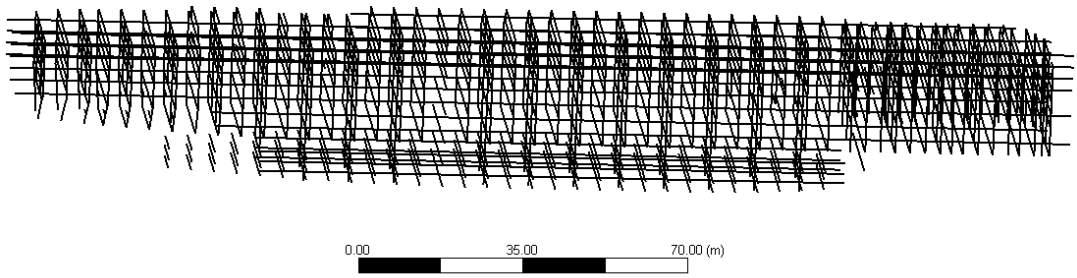

Figure 24, the beam elements of the global model.

A consequence of the lack of local stiffeners is that unreal local deformations of plate fields perpendicular to applied accelerations will occur. For example the side shell of the vessel will bend between web frames when applying a transverse acceleration. This implies that deformations of plate fields that are subjected to perpendicular accelerations only are consistent in way of beams or in connections with other perpendicular plate fields.

A.3.1.1 Global Mesh

The plating is represented by quadrangular and triangular elements with 4 and 3 nodes respectively. The typical mesh size recommended by DNV is equal to vehicle deck spacing (approximately 2,5 meters) if quadratic 6/8 node elements are used. Since linear 3/4 node elements are used in this analysis (quadratic elements not available in the FE-software) at least half that size is required. Therefore a typical mesh size of 1m is used. Special consideration has been given to avoid 3 node triangular elements in general and such elements with sharp corners in particular. That is because such elements may cause errors in the deflexion pattern. The shell elements have five degrees of freedom at each node: translations in the x, y, and z directions and in plane rotations. The sixth degree of freedom about the normal to the shell surface is related to the in-plane components of displacements of the element nodes using a penalty method (set according to ANSYS default [3]).

The pillars, girders, deck beams, webs and ventilation ducts are represented by 2 node beam elements. The beam elements have six degrees of freedom at each node. These include translations in the x, y, and z directions and rotations about the x, y, and z axis.

Since the shell elements do not possess any explicit normal to plane rotational degree of freedom in the nodes special consideration have been given to handle the coupling between beam and shell elements (deck beam or pillar connections to bulkheads). For example if a beam is just attached to a shell in one node the connection will be considered as simply supported. To avoid such weak connections every beam attached to a shell is either overlapping for a number of nodes or perpendicularly attached to another beam which is overlapping a shell. This is illustrated for a typical web frame in figure 25.

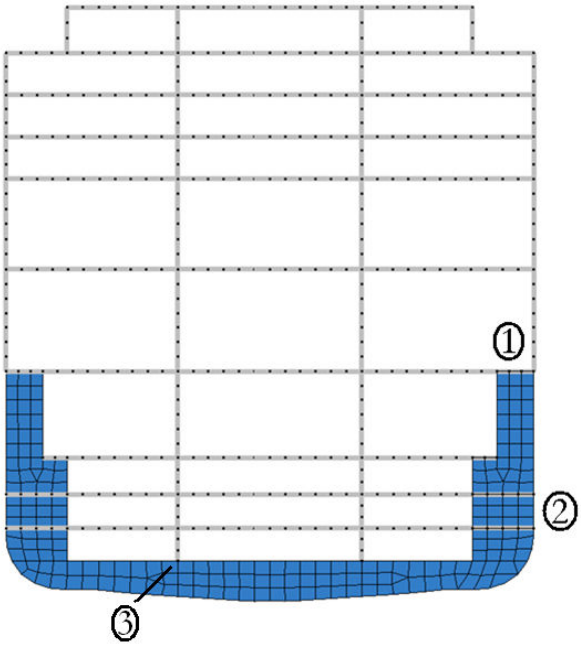

Figure 25, the mesh of a typical web frame with pillars. Marked in the figure is 1: a beam connected to a shell through another beam which is overlapping a shell. 2: beam connected to shell through element overlap. 3: simply supported pillar

In figure 26 an overview of the global mesh is shown. Note the regularity in mesh size and quadrangular dominating mesh shape which are important in order to get reliable deflexion patterns.

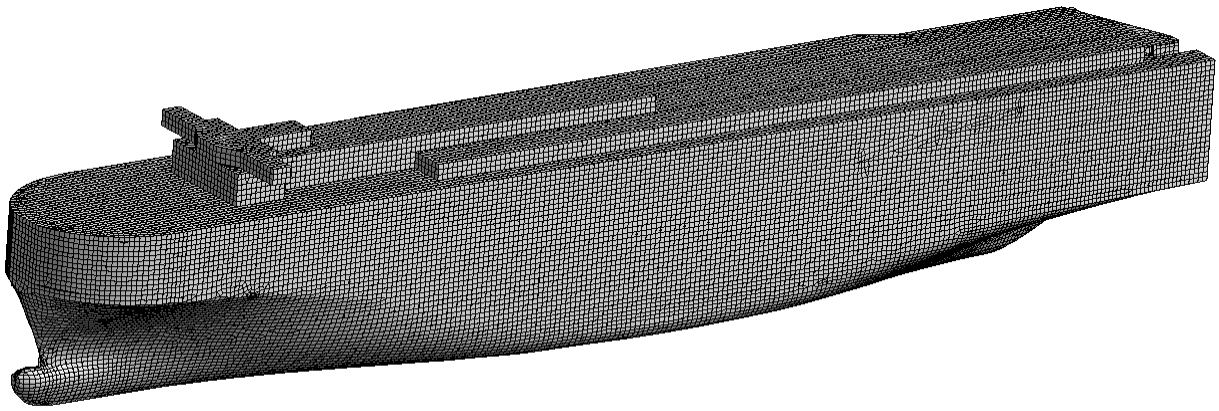

Figure 26, overview of the global model

A.3.2 LOCAL FE MODEL

A local FE model of the racking frame (frame 126, seen in figure 2) is developed separately from the global model using sub-modelling technique. The purpose with the model is to calculate the hot spot stresses in the corners of the bulkhead openings. The extent of the local model is one deck spacing above and below the bulkhead openings and one web spacing in fore and aft direction as shown in figure 27.

The local model includes deck plates, bulkhead plates, deck transversals and girders as well as longitudinal and transverse stiffeners. The local model is exclusively designed by shell elements (same kind as in the global model) using mostly quadrangular and some few triangular elements with 4 and 3 nodes respectively, the typical mesh size is 0,1 m.

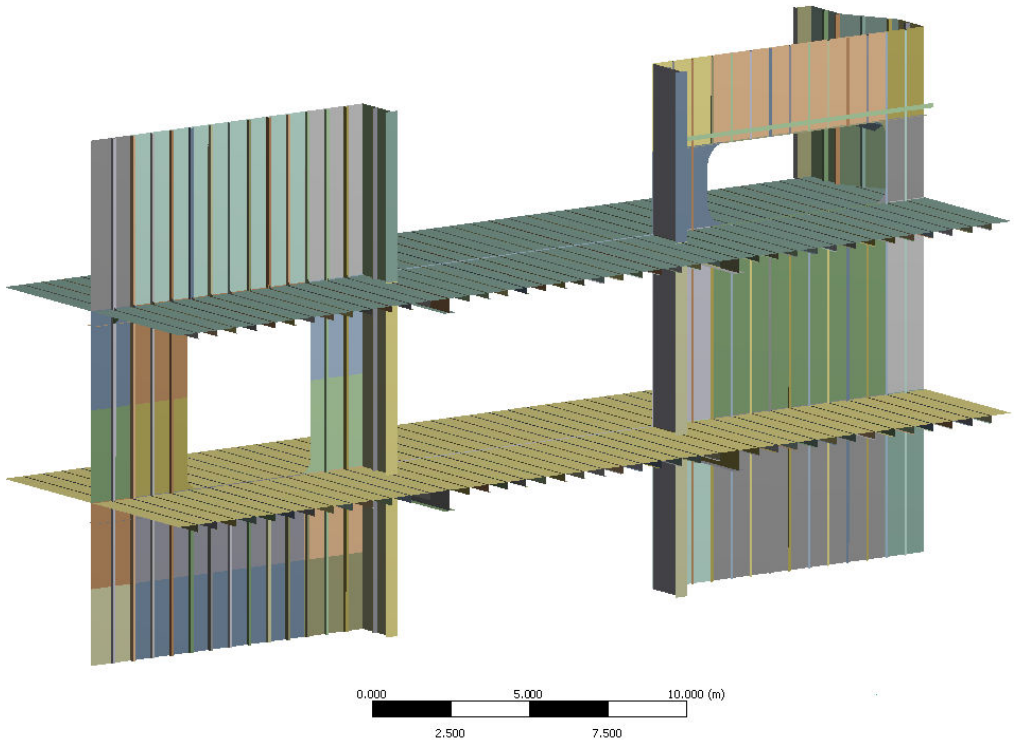

Figure 27, the local FE model of the racking frame

Some relevant details (close to the gauge locations) as for example the brackets adjoining the top of the port side opening has been modelled as can be seen in figure 28.

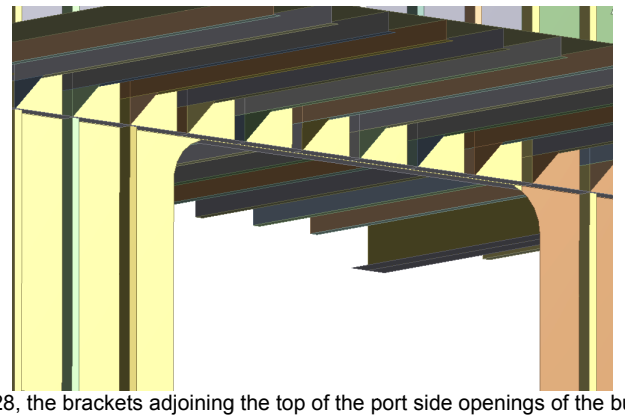

Figure 28, the brackets adjoining the top of the port side openings of the bulkhead

The sub-modelling technique implies that deformations of the global model are applied as loads on the local model. In this case the loads are applied as forced deformations on the boundary nodes of the local

model. In cases where the location of a local node deviates from a global node linear interpolation/extrapolation of the global deformation is used. The boundaries on which the forced deformations are applied are highlighted in figure 29. The philosophy behind the choice of boundaries is to incorporate a consistent three dimensional deformation pattern from the global model, without having any unreal stress concentrations due to the boundaries close to locations of interest.

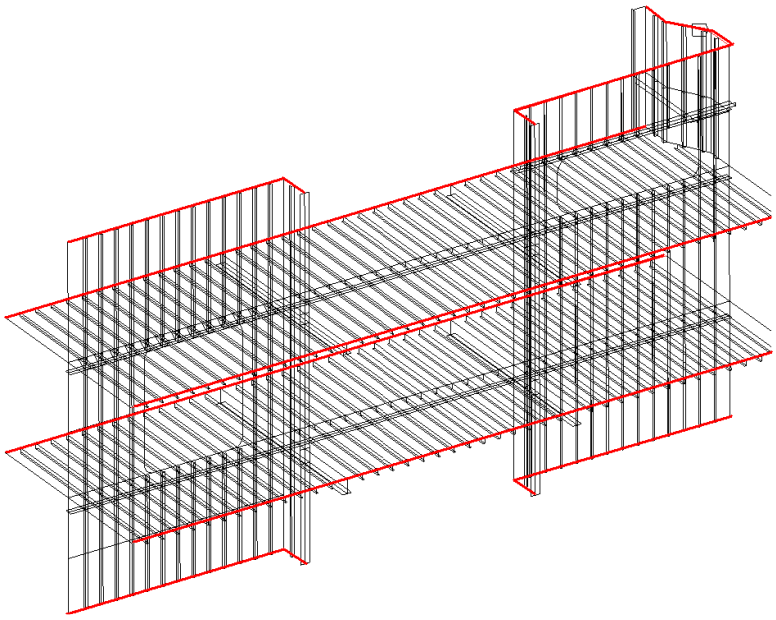

Figure 29, the boundaries of the local model where the forced deformations are applied.

A.3.3 STRENGTH ASSESSMENT

To further compare the LR and DNV boundary approaches stresses according to LR strength assessment criterion will be calculated for Mignon. The procedures defined by LR are intended for the assessment of the strength of the transverse primary structure of Ro-Ro ships using FE methods. The load case that will be evaluated is a "worst case scenario" load case and implies a 30 degrees heeled vessel, fully loaded.

The force components resulting from the 30 degree static heel angle are intended to be sufficient to cater for actual forces resulting from both static and dynamic long term roll motion of the vessel. The stresses obtained from the fine mesh model (local model), in way of free edge openings of transverse bulkheads are not to exceed those in table 1 according to LR.

Table 1, stress criteria for fine mesh (local) model stresses according to LR strength assessment criteria [2].

Corner Connection of Deck & Side Transverses Openings & cut-outs in Deck & Side Transverses Corners of Openings in Transverse Bulkheads Allowable Stresses		
Item	**Average stress over connection**	**Peak Stress (Single element)**
Von Mises Stresses	$0.94\sigma_o$	$1.10*\sigma_o$
where	σ_o is the minimum yield strength of the material	

σ_0 = 360 MPa for the HT-36 steel used in the analysed hot spot locations.

A.3.3.1 healed case 30 degrees using DNV approach model

The full "DNV boundary" model is solved with the LR strength assessment loads. The heeled case loading does include the static gravitational components of all the structural and non structural mass. The loads on decks are represented by the maximum design loads that the ship is designed to carry. See appendix B for detailed information about these loads. The acceleration values are taken as

Vertical component	8,6 m/s^2
Transverse component	5 m/s^2

Equilibrium of forces and moments are obtained by applying forces and moments on the lower hull (below deck 4) as in A.2.3. In this case an equally distributed vertical pressure has to be added to achieve equilibrium in the vertical direction. The balancing forces and moments are shown in Appendix B. The deformations from the global model are applied to the local model as described in A.3.2. In figure 30 the equivalent stresses (von Mises) are plotted for the bulkhead. In the figure the deformations have been magnified 100 times.

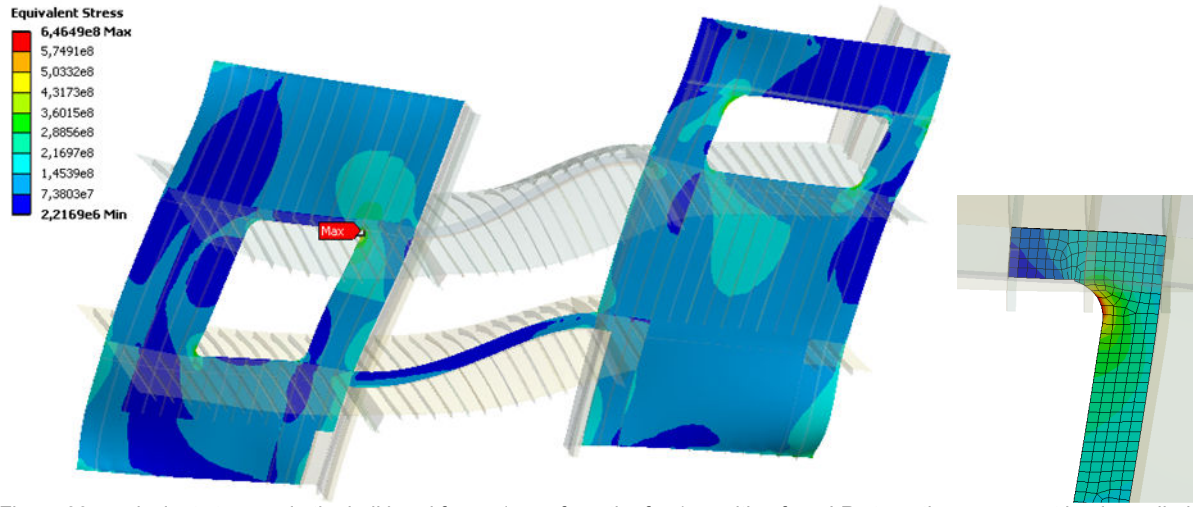

Figure 30, equivalent stresses in the bulkhead frame (seen from the fore) resulting from LR strength assessment loads applied to a DNV boundary FE model. In the right hand side of the figure the detailed stress distribution of the highest stressed location is zoomed.

The maximum stress occurs in the port side of the deck 6 opening and is 646MPa which is higher than allowed (396MPa allowed for single element peak stress).

It is worth mentioning that the same acceleration as applied to the global model should be superpositioned to the local model in order to get a correct approach. But, since the stress deviation between solutions with and without superimposed local acceleration has shown to be smaller than 1% (here 646,3MPa with and 646,5MPa without) for this problem, local superimpositioning of the accelerations will be neglected from the following analysis. This is indicating that the global deformations of the decks have superior influence to the stress distribution of the racking constraining structure. It is therefore generally, of outmost importance that the relative deformations between decks are incorporated properly to the local model.

A.3.3.2. healed case 30 degrees using LR approach model

A "LR boundary" model is also solved with the LR strength assessment loads. The limited model is obtained by constraining the full model against translation and rotation below level of bulkhead deck (deck 6). Equivalent stresses (von Mises) in the local model resulting from this load case are plotted in figure 31. In the figure the deformations have been magnified 100 times.

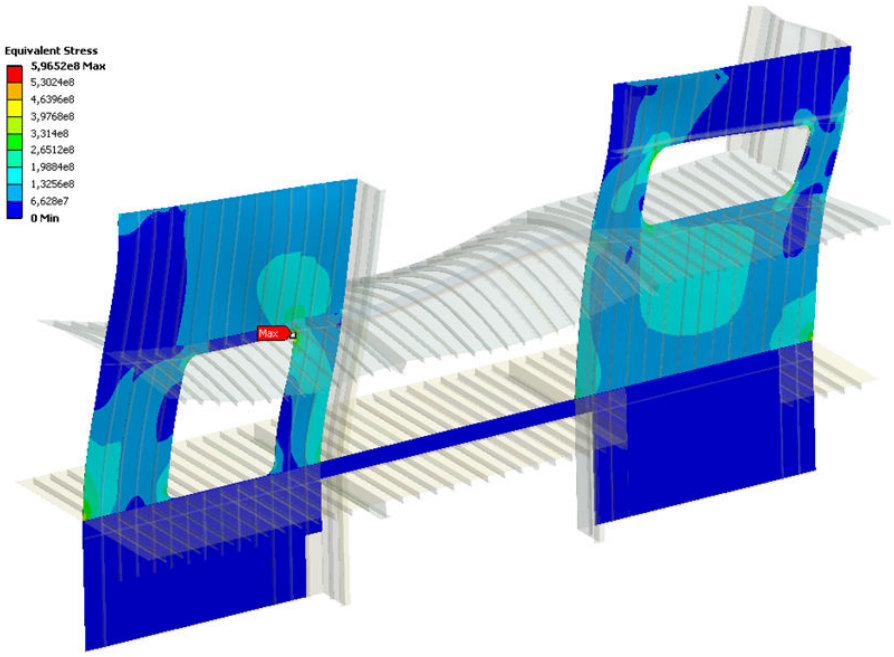

Figure 31, equivalent stresses in the bulkhead frame (seen from the fore) resulting from LR strength assessment loads applied to a LR boundary FE model.

The maximum stress occurs in the port side of the deck 6 opening and is 597MPa which is higher than allowed.

A.3.4. CONCLUSIONS

- The main parameter to stresses in racking structures seems to be relative athwart deformations between decks. Hence, when adopting the sub modelling technique it is of major importance that these deformations are incorporated properly.

- Analogous stress deviation as for the dummy analysis (10%) was found when comparing the two different boundary approaches. This once again indicates that a limited model can be a neat alternative to a full model in order to save work amount. However, the LR boundary approach is according to the results considered to be non conservative. Consequently, it is important to be aware of the limitations of the LR boundary approach if adopting it for calculation of racking induced stresses.

- The corners of the openings of the bulkhead frame do truly seem to be highly stressed. In fact, the stresses resulting from both strength assessments are considerably higher than allowed for classification approval.

Part B: Monitoring of Racking induced stresses

The purpose with this part is to develop a method for monitoring of racking induced stresses. The method is intended to be used for monitoring of the structure as well as for prediction of the structures fatigue life. During the analysis the PCTC vessel Mignon will be used as demonstrator.

Initially inertial as well as gravitational forces acting on a vessel will be analysed. These forces will be applied to the FE model of Mignon that was developed in part A. The intention of this is to simulate hot spot stresses for given time series of motions. Finally the calculated stresses will be evaluated against measured stresses obtained from full scale stress measurements onboard the vessel.

B.1 FORCE ANALYSIS OF THE VESSEL BASED ON MOTION DATA

In this section forces due to motions of vessels in general and m/v Mignon in particular are investigated. The purpose with this section is to analyze the relation and magnitude of the inertial and gravitational forces due to actual motions. The inertial forces as well as the gravitational forces are obtained using rigid body motion theory combined with motion data.

B1.1 DEFINITIONS

Motions of vessels are defined in 6 degrees of freedom as can be seen in figure 32. The translational degrees of freedom are: surge η_1, sway η_2 and heave η_3 and the rotational: roll η_4, pitch η_5 and yaw η_6 which all are defined from the centre of gravity of the vessel.

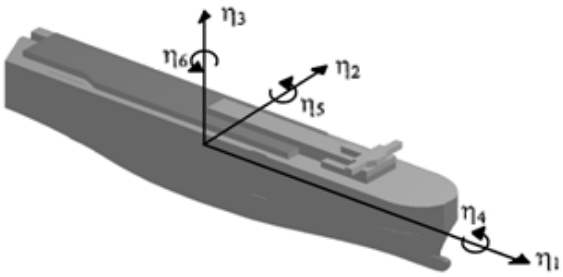

Figure 32, the 6 degrees of freedom of a vessel; the translational: surge η_1, sway η_2 and heave η_3 and the rotational: roll η_4, pitch η_5 and yaw η_6.

For this analysis the definition of positive directions that are shown in table 2 will be used.

Table 2, showing the definition of the positive directions of the 6 degrees of freedom

Degree of freedom	Positive direction
η_1 surge	Forward
η_2 sway	To port
η_3 heave	Upwards
η_4 roll	Starboard side down
η_5 pitch	Bow down
η_6 yaw	Bow to port

In addition to the degrees of freedom of the vessel a local Cartesian coordinate system located in the centre of gravity of the vessel is defined and will be referred to according to figure 33.

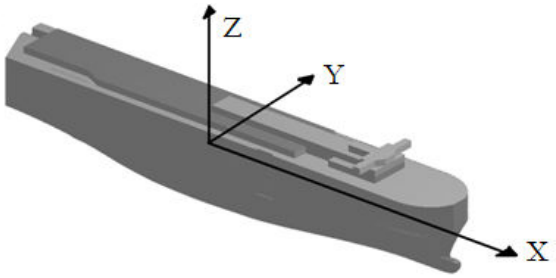

Figure 33, the Cartesian coordinate system defined from the centre of gravity of the vessel.

B.1.2 FORCES DUE TO MOTIONS

Inertial forces in vessels can be derived from the motions in all the 6 degrees of freedom as can be seen in figure 32. To illustrate the counteraction between these degrees of freedom the behaviour of the forces due to roll and sway are analysed. The rolling motion of a vessel η_4 is defined as the rotation around the longitudinal centre line through the centre of gravity and the sway motion η_2 is defined as the translation in athwart direction. When superpositioning these two motions the apparent rolling motion η_{-2+4} around the virtual centre of rolling is obtained. The apparent motion is important because it determines the inertial forces i.e. the acceleration due to the apparent motion is a superpositioning of the accelerations due to roll and sway as illustrated in figure 34.

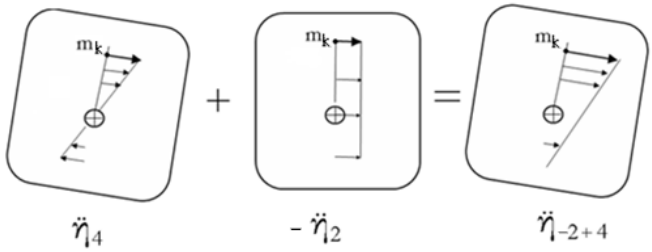

Figure 34, Illustration of transversal inertial forces due to roll + (-)sway accelerations.

The inertial transversal forces F_{y_k} on a mass element m_k (as seen in figure 34) due to roll accelerations is given by

$$F_{y_k} = m_k Z_k \ddot{\eta}_4 \tag{1}$$

where Z_k is the vertical distance from the mass element to the centre of gravity.

The inertial transversal forces due to sway is given by

$$F_{y_k} = -m_k \ddot{\eta}_2 \tag{2}$$

To obtain the complete mass force situation the contribution of the gravitational force must be added. The gravitational force is simple because it does only depend on the rolling angle as illustrated in figure 35

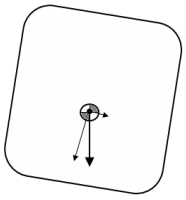

Figure 35, the gravitation and it components due to roll η_4.

The transversal force due to gravitation is calculated according to

$$G_{y_k} = -m_k g \sin \eta_4 \tag{3}$$

where g is the global constant of gravity.

B.1.3 MOTION DATA

The motion recording system *SEAWARE En Route Live* [4] registers the motions of Mignon. The system is recording the motion in every degree of freedom at a sample rate of 10 Hz.

The recorded motions are measured at a location different from the centre of gravity of the vessel. Due to this the motions have to be transformed to the motions of the centre of gravity before proceeding. The recording system is located at the navigation bridge of the vessel, coordinates as seen in table 3.

Table 3, the coordinates of the SEAWARE system that's recording motions, (for CoG according to B.2.3)

$X_{Seaware} = 57$ m
$Y_{Seaware} = 2{,}2$ m
$Z_{Seaware} = 27{,}5$ m

So for example the sway motion η_2 of the centre of gravity is obtained by taking

$$\eta_2 = \eta_{2,\,seaware} + \eta_4 Z_{seaware} \tag{4}$$

When knowing η_2 the transversal motion of any arbitrary position k can be calculated as

$$S_{y_k} = \eta_2 - \eta_4 Z_k \tag{5}$$

In a similar manner the acceleration of any arbitrary position can be calculated as

$$a_{y_k} = -\ddot{\eta}_2 + \ddot{\eta}_4 Z_k - g \sin \eta_4 \tag{6}$$

but, to be able to do this $\ddot{\eta}_2$ and $\ddot{\eta}_4$ have to be obtained numerically from η_2 and η_4.

B.1.4 NUMERICAL DIFFERENTIATION OF RECORDED MOTIONS

To differentiate the finite motion time signals an algebraic different quotient expression is used, i.e. a finite difference approximation [5],

$$\ddot{\eta}_j = \frac{\eta_{j,\ t+\Delta t} - 2\eta_{j,\ t} + \eta_{j,\ t-\Delta t}}{(\Delta t)^2} \tag{7}$$

where $\eta_{j,\ t}$ is the finite time signal of any given motion at the time t and Δt is the finite time step between two motion samples (100 ms).

A necessary condition to be able to differentiate any signal is that the signal is smooth. Otherwise unreal or infinite derivatives will occur. Small errors in the measurement signals (probably caused by finite recording resolution and/or noise) leads to that the recorded signal is not really smooth i.e. have very small spiky oscillations.

These undesired oscillations have a frequency of similar magnitude as the sample rate of the signals. Since the sample frequency is significantly higher than the frequencies of the motion of the vessel these undesired oscillations can be filtered. For this analysis a Fast Fourier Transform (FFT) low pass filter will be applied using MATLAB [6]. The code is shown in appendix A.

To illustrate the behaviour of the FFT filter the rolling motion signal as well as the rolling acceleration before and after the filter is illustrated in figure 36. The figure shows that the FFT filtered roll signal has a very similar behaviour as the unfiltered signal with some exceptions. Noticeable is that the FFT roll signal deviates from the unfiltered signal close to the boundaries. It is thus important to be aware of that FFT filtering could imply errors, especially close to boundaries.

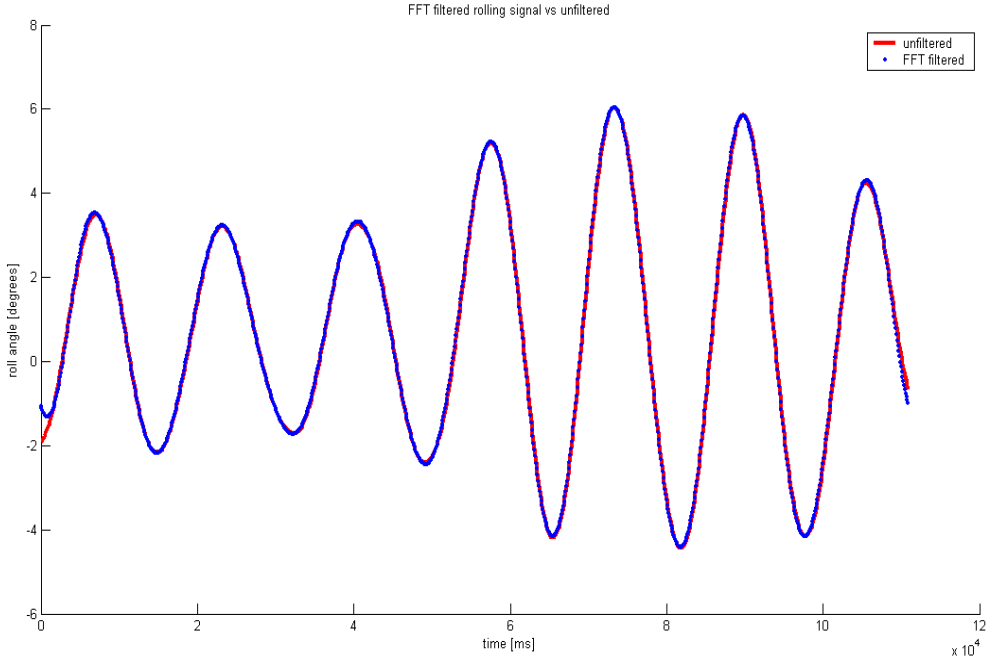

Figure 36, showing η_4 roll signal unfiltered and filtered using FFT low pass filter.

Figure 37 show that the acceleration obtained from the FFT filtered signal is considerably smoother than using the unfiltered signal.

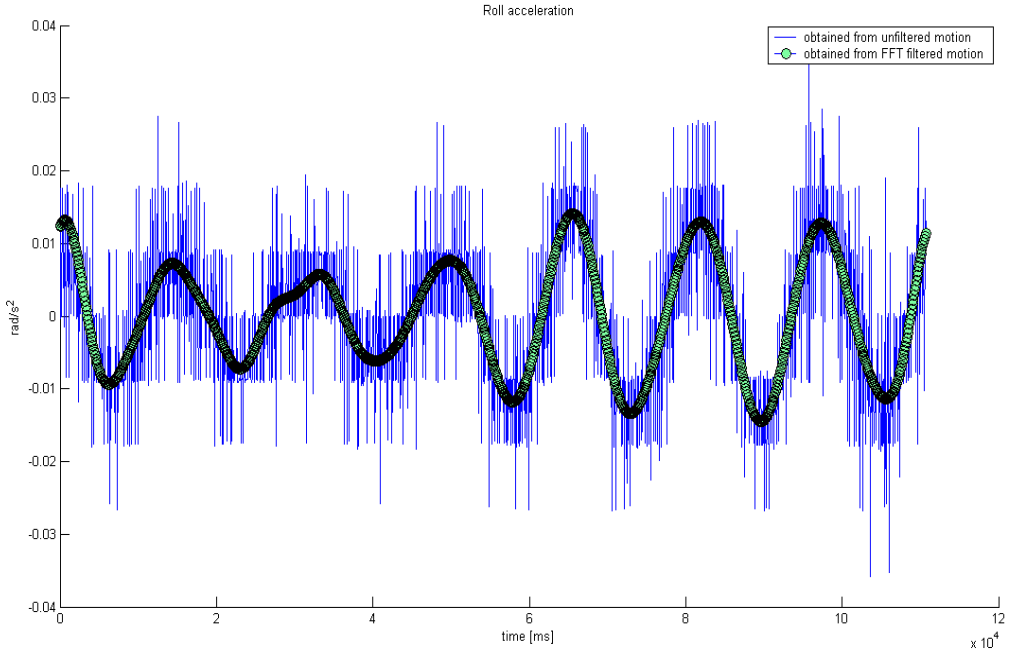

Figure 37, showing $\ddot{\eta}_4$ obtained from motion signal with and without FFT filter.

B.1.5 SUPERPOSITIONING OF FORCES

Now when knowing how to differentiate and superposition motions the acceleration in any given point can be calculated as a function of some or all degrees of freedom.

To illustrate this, the transversal accelerations (a_{y_k}) are calculated for a given time signal as seen in figure 38. The figure is showing the rolling angle η_4, the sway motion η_2, the y acceleration due to gravity, the rolling acceleration $\ddot{\eta}_4$, the sway acceleration $\ddot{\eta}_2$ and the combined transversal acceleration a_{y_k} due to gravity and roll plus sway acceleration at a location Z_k=20 m for any x and y.

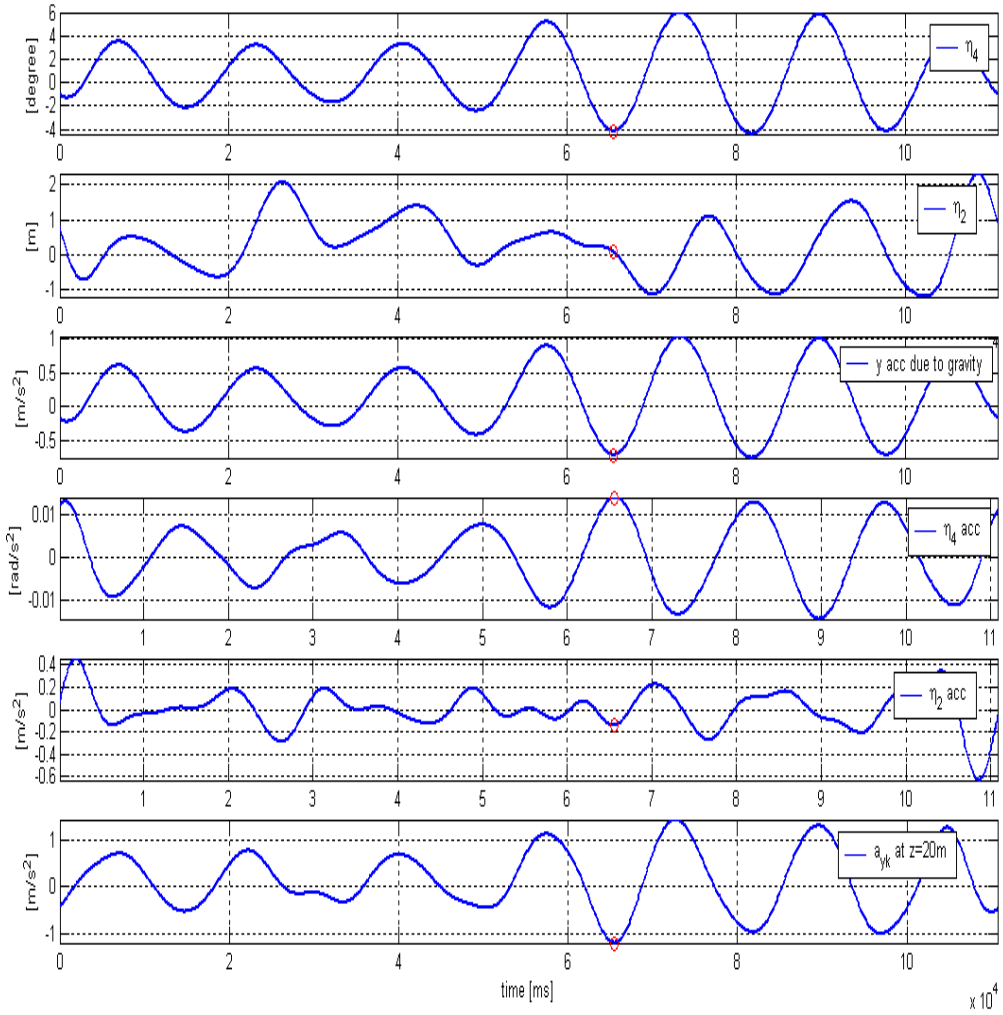

Figure 38, the rolling angle η_4, the sway motion η_2, the transversal acceleration (y-direction) due to gravity, the sway acceleration $\ddot{\eta}_2$, the rolling acceleration $\ddot{\eta}_4$ and a_{y_k} at Z_k = 20 m for any x and y.

The accelerations in the vessel can also be described momentarily. To illustrate this, the horizontal accelerations in the vessel are plotted at the time step marked in figure 38 (approximately after 65 s). Figure 39 is showing the contribution of each transversal acceleration component in the superpositioning of the acceleration situation. In the figure it can for example be seen that the static gravitation component is the dominating part of the horizontal acceleration close to the centre of gravity but that the dynamic effects have considerable effects in the upper part of the vessel.

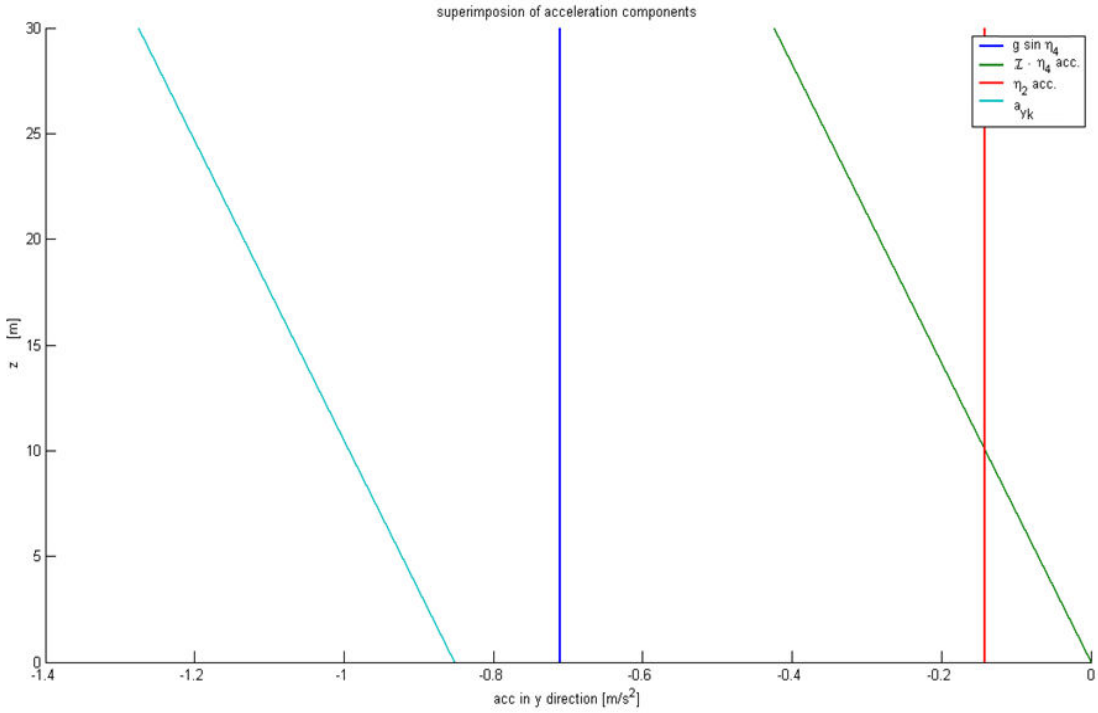

Figure 39, the contribution of the different acceleration components to the total acceleration in the vessel in the y direction due to roll and sway for the particular moment indicated in figure 38.

In a similar manner as for the horizontal accelerations the vertical accelerations a_{z_k} can be calculated. This is carried out for the same period as for the transversal acceleration and can be seen in figure 40 below.

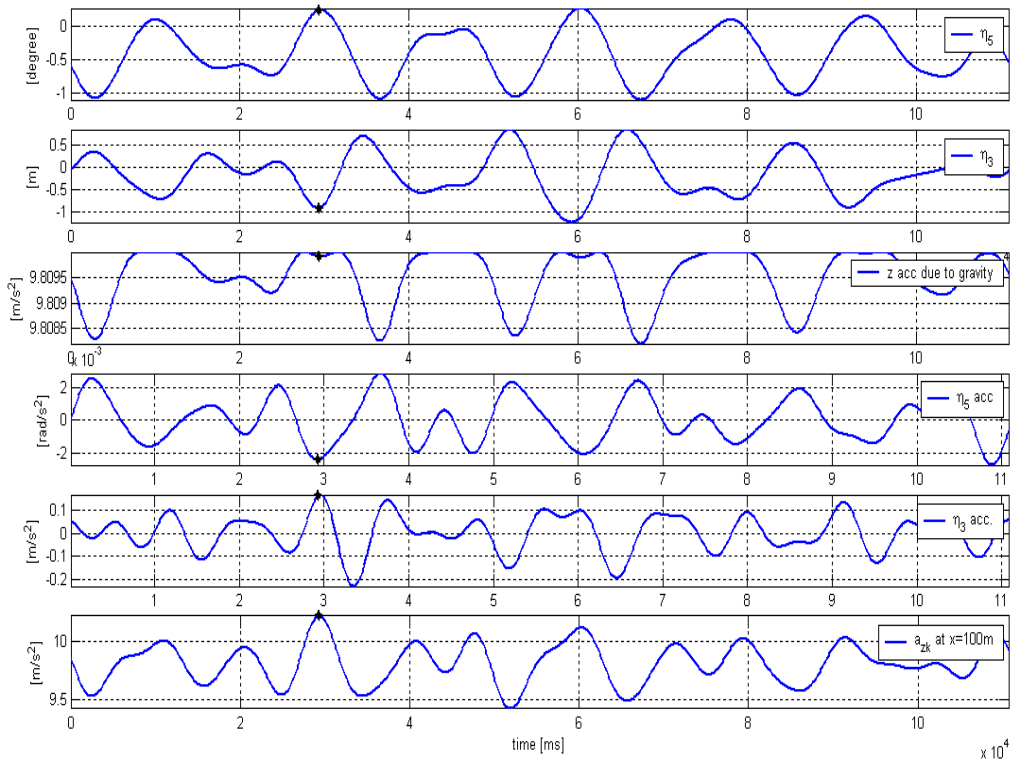

Figure 40, the pitch angle η_5, the heave η_3, acceleration due to gravity, the pitch acceleration $\ddot{\eta}_5$, the heave acceleration $\ddot{\eta}_3$ and the combined acceleration a_{zk} due to pitch and heave acceleration at X_k=100 m for any y and z.

The accelerations in the z-direction can also be plotted momentarily at the time marked in figure 40 (approximately after 28 s). Figures 41 is showing the contribution from pitch and heave as well as the sum of these two components along the vessel, please note that the static gravitation component (9,81m/s²) is subtracted.

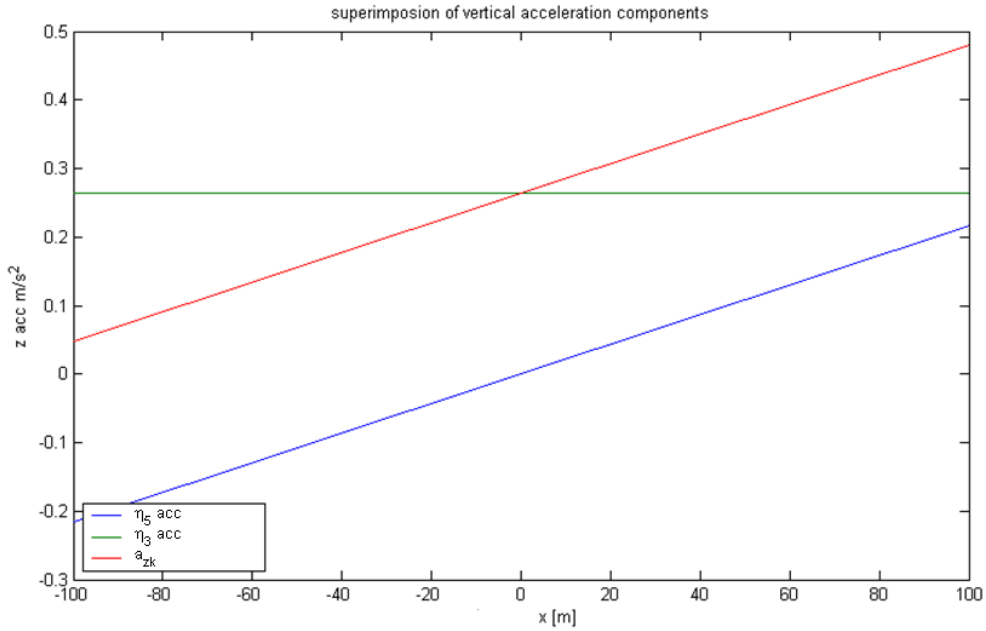

Figure 41, showing the contribution of the different acceleration components to the vertical acceleration in the vessel due to heave and pitch (the static gravitation component of 9,81m/s^2 is subtracted) at the particular moment marked in figure 40.

Finally the yaw motion, yaw acceleration and the transversal accelerations it causes in the fore body (100 m from CoG) is plotted in figure 42 for the same time series as above.

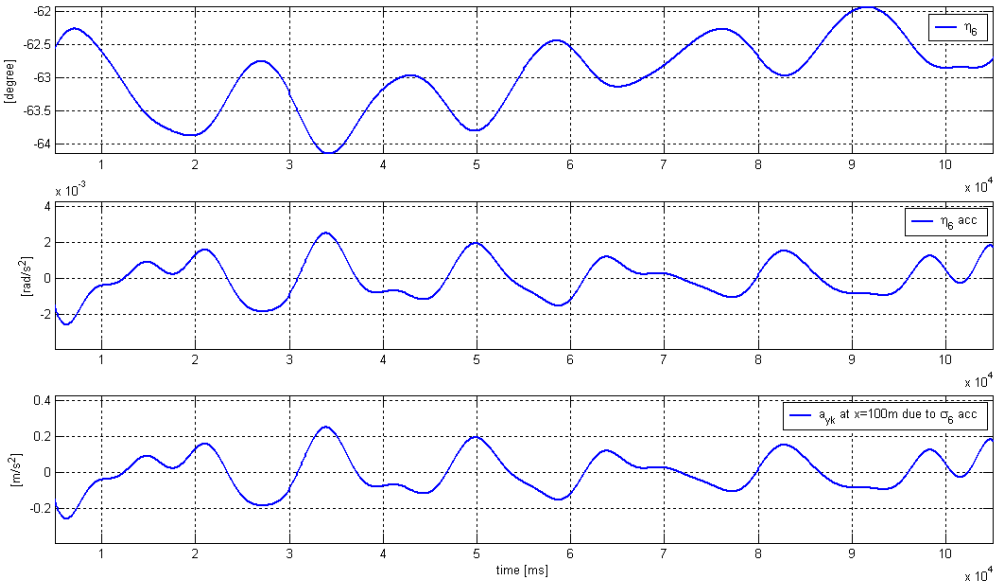

Figure 42, yaw motion η_6 , yaw acceleration $\ddot{\eta}_6$ and the transversal accelerations a_{yk} it causes in the fore body at X = 100m for any y and z.

B.2 SIMULATION OF STRESSES

The global and local FE models of Mignon developed in part A has been used to calculate the stresses in the upper radiuses of the bulkhead openings (frame 126, figure 2). Only inertial and gravitational forces are considered in this analysis. The forces are applied to the full DNV global model according to the method of unit loads, coefficients of influence and linear superpositioning [7]. The theory as well as the implementation of the method is described in the following.

B.2.1 THE THEORY OF UNIT LOADS, COEFFICIENTS OF INFLUENCE AND LINEAR SUPERPOSITIONING

All motion induced structural responses from inertial and gravitational mass forces are assumed to be linear with respect to the motion of every considered degree of freedom. The local stress response due to a combined motion at a certain stress location *i* will be calculated according to

$$\boldsymbol{\sigma}_{\text{tot i}} = \boldsymbol{\sigma}_{\text{g i}} + \boldsymbol{\sigma}_{\text{a i}} \tag{8}$$

where

$\boldsymbol{\sigma}_{\text{g i}}$ = stresses due to gravitational forces

$\boldsymbol{\sigma}_{\text{a i}}$ = stresses due to inertial forces

Generally *i* is a hot spot stress location and $\boldsymbol{\sigma}_{\text{tot i}}$ is a vector containing appropriate stresses of interest for the location, for example *x, y, z*- directional and shear or principal stresses.

The local structural responses from inertial and gravitational mass forces are calculated from the sum of mass forces at various positions/sections *k* multiplied by the influence coefficients representing the stresses at location *i* per unit mass force at section *k*, i.e.

$$\sigma_{a_i} = \sum_k C_{x\,ik} F_{x\,k} + C_{y\,ik} F_{y\,k} + C_{z\,ik} F_{z\,k} \tag{9}$$

$$\sigma_{g_i} = \sum_k C_{x\,ik} G_{x\,k} + C_{y\,ik} G_{y\,k} + C_{z\,ik} G_{z\,k} \tag{10}$$

where

$C_{x\,ik}$ is the coefficient of influence in location *i* due to inertial and/or gravitational unit loads in x direction at section *k* . Hence, $C_{x\,ik}$ can be interpreted as the response relation between the force in one location and the stresses due to this force in another location.

$F_{x\,k}$ is the inertial force in the x-direction at section *k* and $G_{x\,k}$ are the gravitational force in the x-direction at section *k* (etc for other directions). These mass forces are calculated according to

$$F_{x\,k} = m_k a_{x_k} \tag{11}$$

$$G_{x\,k} = m_k g_{x_k} \tag{12}$$

where m_k is the mass of section *k* and a_{x_k} and g_{x_k} is the acceleration/gravitation in x direction affecting the section (etc for other directions).

Depending on the desired resolution on the simulations, the considered degrees of freedom of motions and expected cargo variations the sections *k* has to be chosen properly.

B.2.2 APPLICATION

To simulate the racking induced stresses only transversal forces are considered. In section A.2.4 it was shown that motion induced stresses due to pitch and heave are very small in racking constraining structures. Accelerations due to yaw have also been disregarded since these accelerations are small, especially in the middle of the vessel where the racking frame is located. Obviously better accuracy could be achieved if motions of all degrees of freedom would be considered. However, in order to save work load these simplifications seem to be appropriate for this analysis. Due to this the vessel is sliced deckwise into different sections m_k. Sections are chosen in order to be able to incorporate for variations of cargo as well as for inhomogeneous transversal acceleration field as seen in B.1.5.

In six different load cases unit accelerations a_{y_k} of 1 m /s² is affecting each section m_k separately where k = [1, 6]. The sections are shown in figure 43.

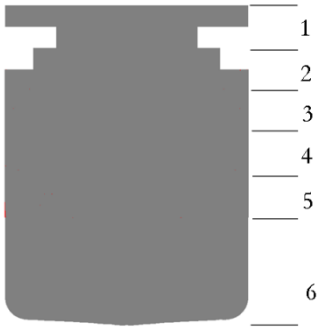

Figure 43, the sections which unit accelerations are affecting in the different load cases

The load caused by the acceleration is implicitly calculated by the FE program according to

$$F_{y\,k} = m_k a_{y_k} \qquad (13)$$

m_k does for this model only include the steel weight of the vessel. So, if cargo or any other loads should be incorporated $F_{y\,k}$ has to be scaled accordingly.

The forces caused by the accelerations are in the different cases balanced with a pressure distributed on the submerged hull (as in figure 10). Moment equilibrium is obtained by applying a distributed moment on the same area (as in section A.2.3). Since absolute balance is difficult to obtain the model is fixed in a single point in the middle of the vessel to avoid rigid body motion. When the model is properly balanced the reaction forces in this point are really small (around 10N) and the location is far enough from the interesting area to be considered to have no influence at all. The balancing reaction forces and moments are shown in Appendix B.

Coefficients of influence $C_{y\,ik}$ representing stresses in the stress locations i = [1,4] (corresponding to figure 2) are calculated for the different load cases as can be seen in table 4. The coefficients of influence are in this case calculated for the first principal stress. This stress is found to be appropriate since it is the by far dominating stress vector in these hot spot locations. The first principal stress is also found suitable since it is considered to represent the stress in the strain gauge locations adequately.

Table 4, coefficients of influence representing stress location *i* resulting from a transversal unit acceleration affecting section *k*.

$C_{y\,ik}$ $^{MPa}/_{kg\,m\,s^{-2}}$	i=1	2	3	4
k=1	1,2945	-3,4856	3,3732	-2,2282
2	7,0618	-18,502	17,597	-11,649
3	7,76	-16,956	15,644	-11,066
4	9,06	-16,27	12,55	-9
5	8,95	-13,162	3,4817	-1,2499
6	-0,25	0,2	-0,3	0,7

In order to calculate a specific load case a_{y_k} has to be determined for k = [1, 6]. For time series of motions the acceleration in each section m_k is calculated according to chapter B.1. In figure 44 accelerations a_{y_k} for k = [1, 6] are shown for a particular moment of time for each section m_k.

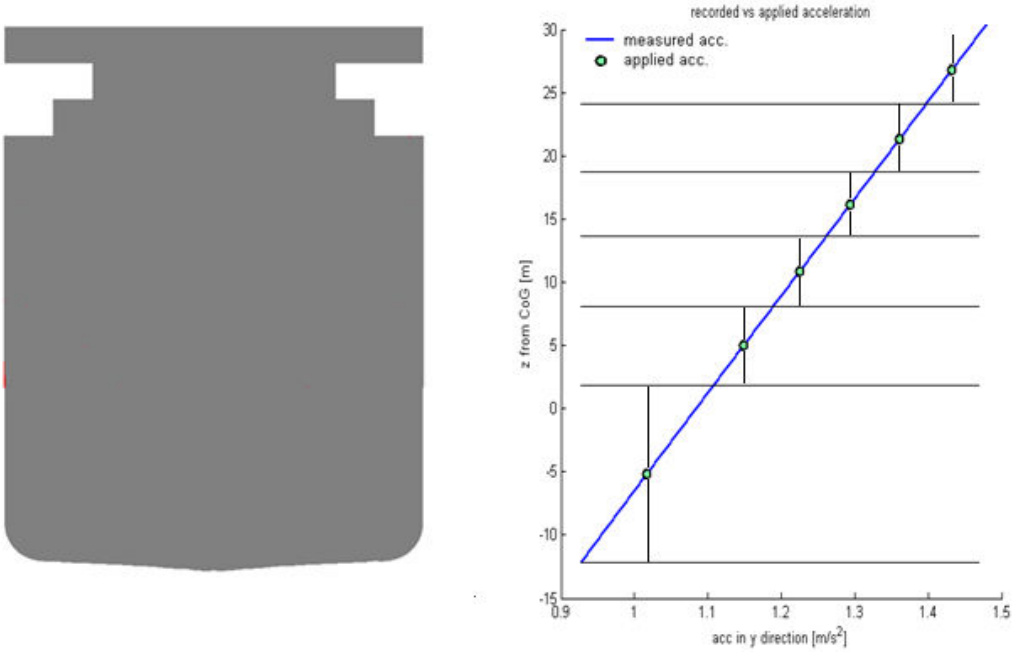

Figure 44, a discrete acceleration distribution as applied in the calculation model compared to a distinct "measured" distribution.

B.2.3 ANALYZED VOYAGE

Finally, time series of stresses are calculated using time series of motions from a particular voyage of Mignon. For this analysis recorded data from the period of 20051201 to 20051208 has been used. The vessel was during that time on voyage from Bremerhaven to the Suez channel. The route during these days is shown in figure 45.

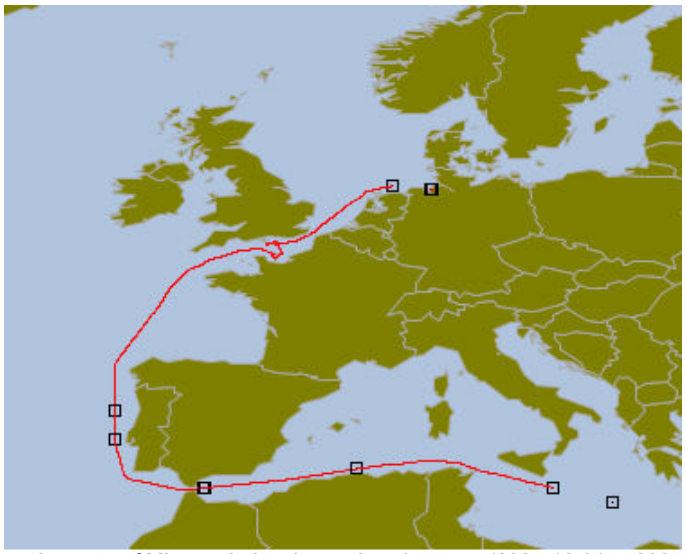

Figure 45, the route of Mignon during the analyzed voyage (2005-12-01 to 2005-12-08)

The weather conditions during this voyage were alternating from 3 to 6 Beufort with waves heights ranging 1-5 meters from various directions.

The loading condition of the vessel during this voyage is shown in table 5.

Table 5, loading condition of Mignon during 2005-12-01 to 2005-12-08

Displacement	32777 tonnes
Draught	7,8 meters
Water ballast	4333 tonnes
Cargo	0

This condition is similar to the light ballast departure condition described in the trim and stability booklet [9] which implies that the centre of gravity should be approximately 12,2 meters above the keel line

B.2.4 EVALUATION

Applying the method as described in B.2.1-B2.2 for the voyage described in B.2.3 the racking induced stresses are calculated. The vessel was free of cargo so no corrections for mass had to be made due to that. However, in the lower hull there was a great deal of non-structural mass like ballast and bunker which normally should be considered. But, since $C_{y\,i6}$ is much smaller than the other coefficients of influence (table 4) no considerable stress deviations could result if ballast, bunker or any fittings would be incorporated to the structural mass. Therefore, no scaling of the mass will be carried out for this voyage.

B.2.4.1 Time series of stresses

The time series are plotted in figure 46 for the same period of time as in chapter B.1.5 where the inertial forces were derived from measured motions. Stress locations 1-4 are located as in figure 2.

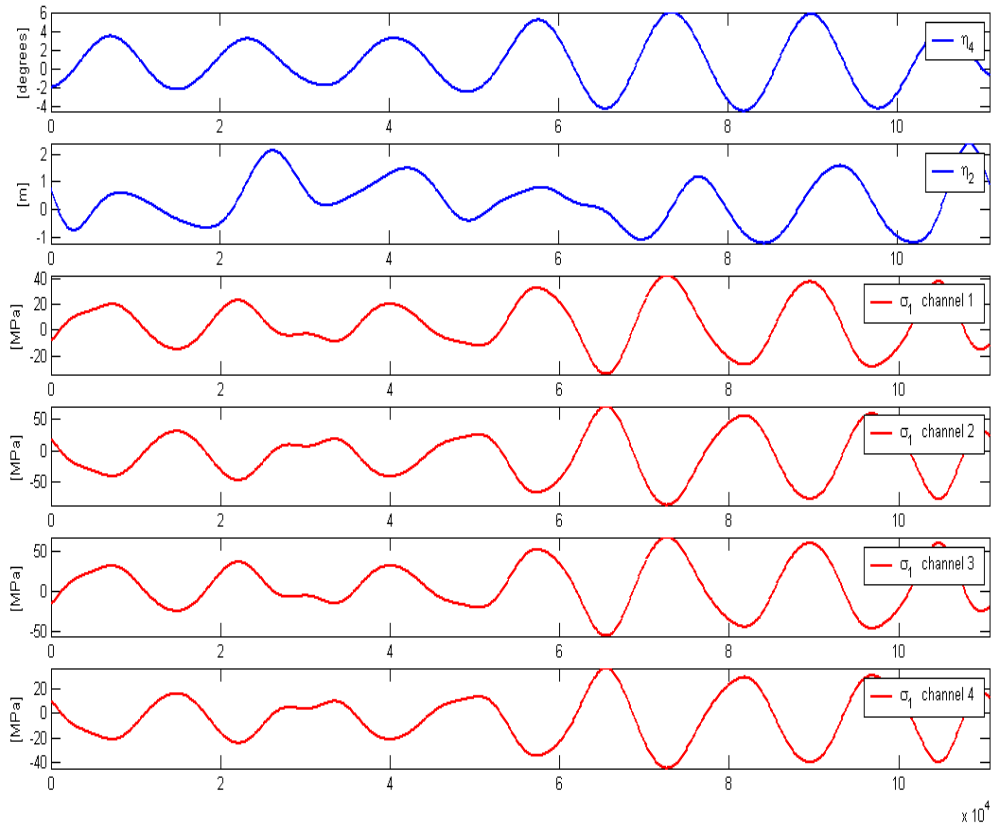

Figure 46, roll motion η_4 and sway motion η_2 as well as the racking induced stresses (first principal stress) in stress location 1-4.

In figure 47 the racking induced stresses as well as the roll and sway motions can be seen for a wider period of time.

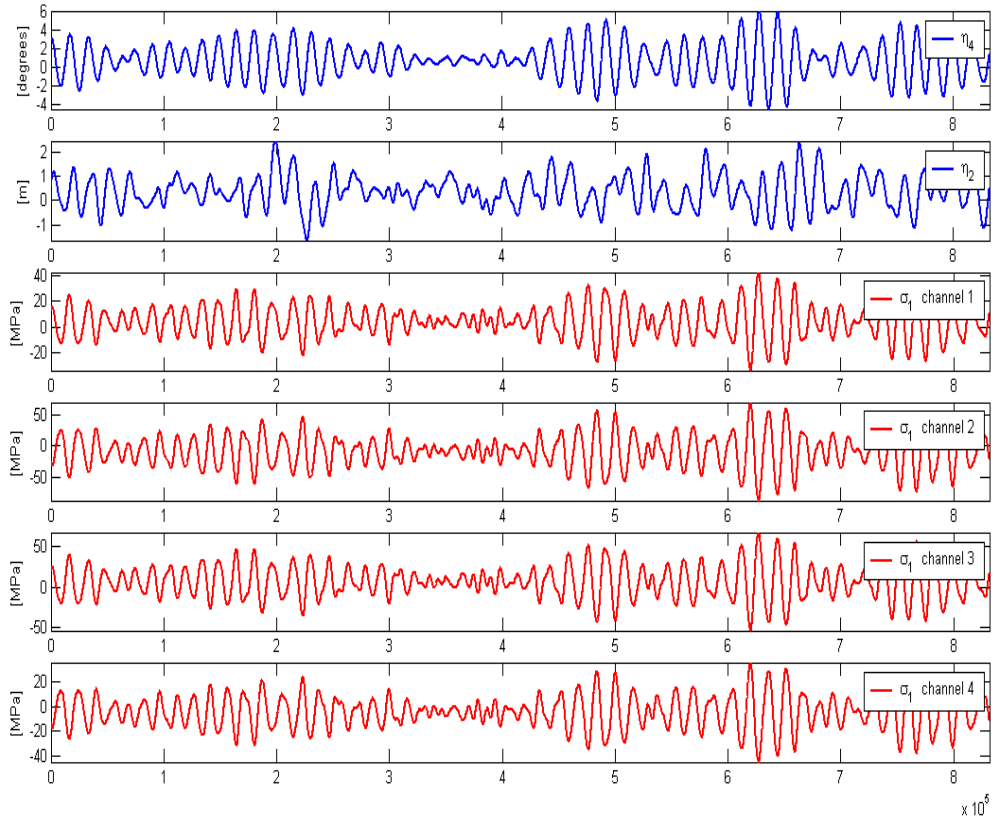

Figure 47, roll motion η_4 and sway motion η_2 as well as the racking induced stresses (first principal stress) in stress location 1-4

Calculated stresses are compared to measured stresses obtained from the strain gauge system installed onboard the vessel.

B.2.4.2 stresses from strain gauge data

Strain gauge data has been recorded as max, mean and min value during every minute for the analyzed voyage. The basic relation between stress and strain is described by the simplified Hook's law [8]

$$\sigma = E\,\varepsilon - E\,\alpha\,\Delta T \qquad (14)$$

where σ is the stress, E is the General Young's modulus, ε is the strain, α is the thermal coefficient of expansion and ΔT is the changes in temperature. The influence of temperature is considered to have minor influence for this application and will therefore be neglected.

Because strain gauges measure changes of deformation in a structure, the measured stresses may not necessarily represent the true stress level in the structure. As an example, if the actual stress level in the structure is -100N/mm² (compression) when the strain gauge is set-up (i.e. the gauging reading is zero) then when the gauge reading is 200N/mm² (tension), the actual stress in the structure is only 100N/mm² (tension) because the reference value is wrong.

However, the measured stress range (max-min) during a minute does represent the true "racking induced" stress range (except for other measurement errors) and will therefore be used for this analysis.

Unfortunately, the strain gauge system suffers from a calibration error, which is confirmed by the installation engineer responsible for the stress measurement system [10]. The error causes a quite large magnification error on the dynamic ranges. Due to this error, speculations regarding the level correlation between measured and calculated stresses are considered superfluous.

B.2.4.3 Calculated stress ranges vs. Measured

To compare the calculated stresses with the measured the racking induced stress ranges are calculated from time series. According to the equipment information both systems (strain gauge and motion data) should be time calibrated against GPS. Unfortunately there seems to be a phase lag between the signals of just below two minutes. For the following analysis the acceleration ranges will be calculated with a phase lag to the strain gauge data in order to get the best possible correlation between the signals (+1 min and 40 sec seems to be a good choice, configured visually). In figure 48 the calculated stresses can be seen for location 1-4 as well as the measured stresses for the same locations.

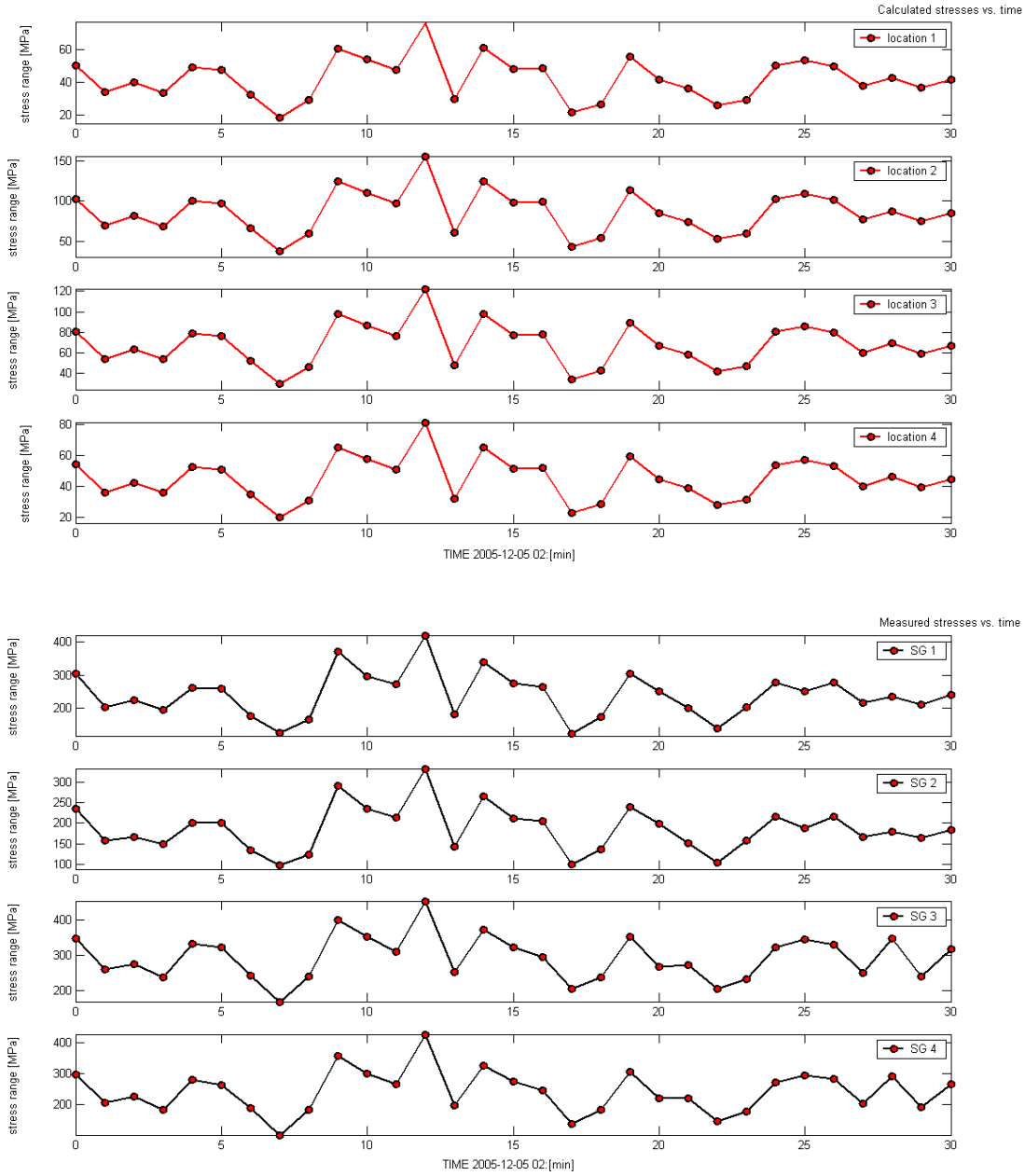

Figure 48, calculated stresses compared to measured stresses for stress location 1-4.

Due to the measurement calibration error, the implementation of the method for monitoring of racking induced stresses could not be quantitatively verified here. However, when comparing the calculated stresses with the measured, the stress range oscillations appear to be qualitatively consistent. This should verify that the method is genuine and appropriate for monitoring of racking induced stresses.

GENERAL CONCLUSIONS

For Pure Car and Truck Carriers (PCTC) the general strength problem is transverse racking. Racking induced stresses are generally due to motions, which imply that material fatigue is the main problem. In the first part of this thesis different approaches for direct calculations of racking induced stresses have been analysed. In the second part a method for monitoring of these stresses has been developed and implemented to the Wallenius Marine PCTC Mignon based on measured motions.

- When constructing FE models for direct calculations of racking induced stresses various boundary conditions and loads could be applicable. If only locations above the bulkhead deck are of interest a limited FE model clamped below main deck could be a neat and time efficient choice (LR approach). This is due to that PCTC vessels in general are much stiffer in athwart direction below bulkhead deck. But, if the whole vessel is of interest a complete FE model is required. Such model is preferably solved with a distributed external pressure on the lower hull balancing the racking force and moment (DNV approach).

- When constructing local models for calculation of detailed stress distributions it is of outmost importance that the relative deformations between decks are incorporated properly. Preferably forced deformations are applied to a local model at least one deck spacing above and below the interesting spots as well as one web spacing in fore and aft direction.

- Inertial and gravitational forces caused by the rolling motions have been shown to be the major contributor to stresses in racking constraining structures.

- The method of unit loads, coefficients of influence and linear superpositioning has been efficient for simulation of stresses, based on measured motions. The method implies solving the FE model for unit accelerations affecting different divisions of the vessel separately. Depending on the desired resolution on the simulations and expected cargo variations these divisions has to be chosen in order to incorporate for alternating inertial forces. A proper simplification for simulation of stresses in racking constraining structures of PCTC vessels seems to be to only consider mass forces due to roll and sway.

- Simulation of racking induced stresses through time series of motions of the PCTC Mignon has shown to be qualitatively consistent when comparing with measured stresses. This indicates that a full scale live stress monitoring system is achievable by applying this method properly. As future work new refined measurements are desirable in order to calibrate and validate the stress monitoring method quantitatively.

- Finally, the corners of the openings of the bulkhead frame of Mignon do truly seem to be highly stressed. Actually, stresses resulting from the LR strength assessment that was carried out were higher than allowed for classification approval. The simulation of time series does also indicate relatively high stresses even for moderate racking conditions in terms of weather and cargo. Therefore, continuous inspections of these stress locations are recommended.

THANKS

Special thanks to Andreas Söderberg and Mikeal Huss at Wallenius Marine for an appreciated supervision of this analysis. Another special thanks to Anders Rosén at KTH for his superb guidance throughout the whole master thesis course.

REFERENCES

1. Classification notes No. 31.2 *Strength Analysis of Hull Structure in Roll on/Roll of Ships and Car Carriers*. Det Norske Veritas, Høvik, Norway, April 2006

2. *Ro-Ro Ships Direct Calculation Procedure,* Draft Version: Pre-Release 01.03. Lloyd's Register, Class Computational Services Group, April 2004

3. ANSYS, ANSYS Workbench SP1, Copyright 2007, SAS IP, inc

4. Seaware En Route Live, Seaware AB, PO Box 1244, Nacka Strand Sweden

5. *Computational Fluid Dynamics*, John D. Anderson, JR. McGraw-Hill International Editions 1995

6. MATLAB, Student Version 6.5.0. 1924 Release 15 Copyright 1984-2002

7. *Prediction of combined Long-term Wave Induced Stresses and Corresponding fatigue Damage in a Ship's Bottom Girder*, Mikael Huss and Gustaf Lindvall 1990. Royal Institute of Technology (KTH), Department of Naval Architecture.

8. *Handbok och Formelsammling i Hållfasthetslära,* Royal Institute of Technology (KTH), Department of Solid Mechanics, KTH, Bengt Sundström, 1998

9. H04C503 M/V Undine (sister vessel to Mignon) Trim and Stability booklet

10. David Smith. Strainstall UK Limited, 9-10 Mariners Way, Cowes, Isle of Wight, P031

APPENDIX A, MATLAB CODE

```
function [data]=ReadRecViewerTimeSeries(filename);

if nargin<1,
        [fname, path] = uigetfile('*.*', 'Select file:');
        if path==0,
                error('Cancelled operation');
                return
        end
        fullname=[path,fname];
elseif nargin==1,
        fullname=filename;
end
fid=fopen(fullname,'r');
data.filename = fullname;
data.info = fgets(fid);
header = fgets(fid);

[mtx] = (fscanf(fid,'%f',[7 inf]))';
time=mtx(:,1) %ms
heave=mtx(:,2); %m
pitch=mtx(:,3); %_deg
roll=mtx(:,4);%_deg
sway=mtx(:,5);%_m
surge=mtx(:,6);%_t
yaw=mtx(:,7);%_deg

% Motion measure position
mp.x = 167.0;,mp.y = 2.245;,mp.z = 39.48; %from AP and CL
% CG position
cg.x = 110; ,cg.y = 0; ,cg.z = 12.2;
% calc in CG
dx = mp.x - cg.x; ,dy = mp.y - cg.y; ,dz = mp.z - cg.z;

t=1
tt=length(roll)
n=1
ROLL=mtx(t:tt,4)

% Definition of the boundary frequencies of the FFT filter
freq1  =0.0;        %lower frequency
freq2  = 0.1;       % upper frequency
cutoff = [freq1 freq2];
plotta = 0;
[ROLL]=fft_bandpass(ROLL,t:tt,cutoff,plotta);

n=1
ROLL=pi/180*ROLL;
 RBIS=[];
  for ii = 1+n:(length(ROLL)-n);
     Rbis=(ROLL(ii+n)-2*ROLL(ii)+ROLL(ii-n))/((time(ii+n)-time(ii))^2);
     RBIS=[RBIS Rbis];
 end
 RBIS=RBIS*10^6; %ms2 => s2
 gravacc=sin(ROLL)*9.81;

SWAY=mtx(t:tt,5);
freq1  =0.0;
freq2  = 0.1;
cutoff = [freq1 freq2];
plotta = 0;
[SWAY]=fft_bandpass(SWAY,t:tt,cutoff,plotta);
```

```
n=1;
 SBIS=[];
 for ii = 1+n:(length(SWAY)-n);
     Sbis=(SWAY(ii+n)-2*SWAY(ii)+SWAY(ii-n))/((time(ii+n)-time(ii))^2);
     SBIS=[SBIS Sbis];
 end

SWAY=SWAY+dz*ROLL;
 SBIS=SBIS*10^6; %ms2 => s2
SBISCoG=SBIS+dz*RBIS;

ACC=[];
for Z= [39000 33480 28370 23040 17160 7000]*10^-3-cg.z;
    acc=gravacc(1:length(SBISCoG))'+SBISCoG-RBIS*Z;
    ACC=[ACC;acc];
end

c1=[1.2945 7.0618 7.76 9.06 8.95 -0.25]; % coeff. of influence stress location 1 etc..
c2=[-3.4856 -18.502 -16.956 -16.27 -13.162 0.2];
c3=[3.3732 17.597 15.644 12.55 3.4817 -0.3];
c4=[-2.2282 -11.649 -11.066 -9 -1.2499 0.7];

C=[c1;c2;c3;c4];
stress=C*ACC;

corr=0; % time correction
for sg=1:4
  STRESSRANGE=[];
  start=20+corr;
    platts=start:600:length(stress(sg,:))
    for i=[3:63]
        [stressmax,I]=max(stress(sg,(platts(i):platts(i+1)-1)))
        [stressmin,J]=min(stress(sg,(platts(i):platts(i+1)-1)))
        stressrange=stressmax-stressmin
        STRESSRANGE=[STRESSRANGE stressrange]
    end

    subplot(4,1,sg),plot(0:length(STRESSRANGE)-1,STRESSRANGE,'-
o','LineWidth',2,'MarkerEdgeColor','k','MarkerFaceColor',[.49 1 .63],'MarkerSize',6), axis tight
ylabel('stress range [MPa]')
end
title('SG 1- 4 ,stress range vs time')
xlabel('TIME 2005-12-05 02:[min]')
```

APPENDIX B, APPROXIMATIONS

Table b1, estimated equivalent thickness of vertical structures.

Structural element	Plate thickness [mm]	stiffner	cross section area [mm2]	equivalent stiffner spacing [mm]		Equivalent thickness of "smoothed" stiffner	equivalent thickness [mm]
side shell below deck 6	16	250x30x10/15	2800	4800/5=960		2,916666667	19
side shell deck 6-8	10,5	200x90x9/14	3060	4800/5=960		3,1875	13,5
side shell abowe deck 8	9	150x90x9	2160	4800/5=960		2,25	11,25
long. bhd. above deck 6	10	150x90x12	2160		800	2,7	12,7
long. bhd. below deck 6	10,5	200x90x9/14	3060		800	3,825	14,325
long. bhd. below deck 4	11,5	200x90x9/15	3060		800	3,825	15,325
transversal bulkheads above deck 6	10	150x90x9	2160		750	2,88	12,88
transversal bulkheads below deck 6	12	150x15	2250		750	3	15
bottom floor	15	-					30*
bottom girder 5625 of CL	20	250x90x10/15	3850		800	4,8125	24,8125
long bhd. 5625 of CL	10	150x90x9	2160		800	2,7	12,7
bottom girder & long bhd. on CL	17	-					17

*Generally the floor spacing is about half the web spacing, to incorporate this the equivalent thickness of the bottom floor is doubled.

Table b2, estimated equivalent density of decks.

Structural element	Plate thickness [mm]	Stiffner	cross section area [mm2]	stiffner spacing [mm]	Equivalent thickness of "smoothed" stiffner	added thickness from movable decks	equivalent density factor
Deck 1	13	250x90 x10/15 (L)	3850	750	5,133333333		1,394871795
Deck 2	6	125x60x6/8 (I)	1710	750	2,28		1,38
deck 3	6	125x60x6/8 (I)	1710	750	2,28		1,38
deck 4	10	200x90x9/14 (L)	3060	750	4,08		1,408
deck 5 (movable)	6	125x60x6/8 (I)	1710	750	2,28		
deck 6 (aft fr. 126)	13,5	350x100x12/17 (L)	5900	750	7,866666667	8,28	2,196049383
deck 6 (fore fr. 126)	10,5	250x90x10/15 (L)	3850	750	5,133333333	8,28	2,277460317
deck 6 (average)	12						2,23675485
deck 7 (fixed)	8	150x90x9	2160	750	2,88		1,36
deck 7 (movable)	6	125x60x6/8 (I)	1710	750	2,28		
deck 8	10	200x90x9/14 (L)	3060	750	4,08	8,28	2,236
deck 9 (fixed)	8	150x90x9	2160	750	2,88		1,36
deck 9 (movable)	6	125x60x6/8 (I)	1710	750	2,28		
deck 10	6	125x60x6/8 (I)	1710	750	2,28	8,28	2,76
deck 11	6	125x60x6/8 (I)	1710	750	2,28		1,38
deck 12	6	125x60x6/8 (I)	1710	750	2,28		1,38
upper deck	9	150x90x9	2160	750	2,88		1,32
garage deck	6	175x75x7	1750	750	2,333333333		1,388888889
deck house	9	125x75x7	1400	750	1,866666667		1,207407407

* The movable decks are assumed to be hoisted during the analyzed voyage and the structural weight from these decks are incorporated as added density at the fixed deck above.

Table b3, Mass of cargo (very heavy loading) as well as weight of hoistable decks [9]

	deadweight [Ton]	hoistable deck weight [Ton]	added mass [Ton]
deck1	253		253
deck2	448		448
deck3	370		370
deck4	2128		2128
deck5		311	0
deck6	5148		5459
deck7		588	0
deck8	3256		3844
deck9		609	0
deck10	1412		2021
deck11	1424		1424
deck12	767		767
deck13	391		391

Table b4, applied forces on submerged hull to obtain equilibrium.

load case	x [N]	y [N]	z [N]	x mom. [Nm]	y mom. [Nm]	z mom. [Nm]
section 1	0	246489	0	-8677778	-637	7843027
section 2	0	1431142	0	-44186394	-3387	-3356860
section 3	0	1517867	0	-39612405	-2980	712311
section 4	0	1766042	0	-38354566	-1843	3354260
section 5	0	2207123	0	-35594968	-2665	7531591
section 6	0	6600401	0	-30695553	-2221	-20102884
"DNV", strength assesment	734	147258800	253284366	-2121455062	-638923483	371364866

APPENDIX C, STRAIN GAUGE INFORMATION

Channels 1 to 4 are measured with resistive strain gauges as can be seen in figure 2; CEA-06-W250A-350 from Vishay Micro Measurements [5] is used.

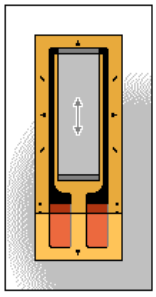

Dimensions	mm
Carrier* Length	16.0
Carrier Width	8.6
Carrier Thickness	0.13
Grid Length	5.84
Grid Width	3.18
Matrix Length	11.2
Matrix Width	4.3